Applied Microbiology and Biotechnology (2018) 102:6001–6021
https://doi.org/10.1007/s00253-018-9009-2

BIOTECHNOLOGICALLY RELEVANT ENZYMES AND PROTEINS

CfPDIP1, a novel secreted protein of *Colletotrichum falcatum*, elicits defense responses in sugarcane and triggers hypersensitive response in tobacco

N. M. R. Ashwin[1] · Leonard Barnabas[1] · Amalraj Ramesh Sundar[1] · Palaniyandi Malathi[1] · Rasappa Viswanathan[1] · Antonio Masi[2] · Ganesh Kumar Agrawal[3,4] · Randeep Rakwal[3,4,5]

Received: 18 November 2017 / Revised: 3 April 2018 / Accepted: 8 April 2018 / Published online: 4 May 2018

Abstract

Colletotrichum falcatum, a hemibiotrophic fungal pathogen, causes one of the major devastating diseases of sugarcane—red rot. *C. falcatum* secretes a plethora of molecular signatures that might play a crucial role during its interaction with sugarcane. Here, we report the purification and characterization of a novel secreted protein of *C. falcatum* that elicits defense responses in sugarcane and triggers hypersensitive response (HR) in tobacco. The novel protein purified from the culture filtrate of *C. falcatum* was identified by MALDI TOF/TOF MS and designated as *C. falcatum* plant defense-inducing protein 1 (CfPDIP1). Temporal transcriptional profiling showed that the level of CfPDIP1 expression was greater in incompatible interaction than the compatible interaction until 120 h post-inoculation (hpi). EffectorP, an in silico tool, has predicted CfPDIP1 as a potential effector. Functional characterization of full length and two other domain deletional variants (CfPDIP1ΔN1-21 and CfPDIP1ΔN1-45) of recombinant CfPDIP1 proteins has indicated that CfPDIP1ΔN1-21 variant elicited rapid alkalinization and induced a relatively higher production of hydrogen peroxide (H_2O_2) in sugarcane suspension culture. However, in *Nicotiana tabacum*, all the three forms of recombinant CfPDIP1 proteins triggered HR along with the induction of H_2O_2 production and callose deposition. Further characterization using detached leaf bioassay in sugarcane revealed that foliar priming with CfPDIP1Δ1-21 has suppressed the extent of lesion development, even though the co-infiltration of CfPDIP1Δ1-21 with *C. falcatum* on unprimed leaves increased the extent of lesion development than control. Besides, the foliar priming has induced systemic expression of major defense-related genes with the concomitant reduction of pathogen biomass and thereby suppression of red rot severity in sugarcane. Comprehensively, the results have suggested that the novel protein, CfPDIP1, has the potential to trigger a multitude of defense responses in sugarcane and tobacco upon priming and might play a potential role during plant-pathogen interactions.

Keywords *Colletotrichum falcatum* · Elicitor · Effector · Hypersensitive response · Sugarcane · Red rot

Electronic supplementary material The online version of this article (https://doi.org/10.1007/s00253-018-9009-2) contains supplementary material, which is available to authorized users.

✉ Amalraj Ramesh Sundar
rameshsundar_sbi@yahoo.co.in

[1] Plant Pathology Section, Division of Crop Protection, Indian Council of Agricultural Research - Sugarcane Breeding Institute, Coimbatore, Tamil Nadu 641 007, India

[2] Department of Agronomy, Food, Natural Resources, Animals and Environment, University of Padova, Padova, Italy

[3] Research Laboratory for Biotechnology and Biochemistry, Kathmandu, Nepal

[4] GRADE (Global Research Arch for Developing Education) Academy Private Limited, Adarsh Nagar-13, Birgunj, Nepal

[5] Faculty of Health and Sport Sciences, and Tsukuba International Academy for Sport Studies (TIAS), University of Tsukuba, Tsukuba, Ibaraki, Japan

Introduction

Sugarcane is one of the important commercial crops cultivated in more than 100 countries for the production of sugar, ethanol, and other by-products (http://www.fao.org/faostat/en/#data/QC). *Colletotrichum falcatum*, a hemibiotrophic fungal pathogen that causes red rot, poses a serious threat to sugarcane production in many tropical and subtropical countries (Singh and Lal 2000). The disease has been responsible for a considerable reduction of cane yield (30–100%) and sucrose recovery (25–75%) (Viswanathan 2012). Complex polyploidy and absence of whole genome information of sugarcane have hampered the efforts of breeding for achieving durable red rot resistance (Sundar et al. 2015; Viswanathan 2017). Disease management practices involving fungicidal applications were not found to be effective at the grand growth phase of the crop. Nevertheless, the application of few biotic and abiotic resistance inducers has been successfully demonstrated to induce systemic resistance against red rot of sugarcane (Ashwin et al. 2017a).

Biotic resistance inducers or pathogen-derived signatures predominantly encompass cell structure-associated biomolecules and secreted proteins (Zhang and Zhou 2010; Böhm et al. 2014). Of these, the well-conserved, essential pathogen signatures, which are often recognized by a broad range of plants are called as "pathogen-associated molecular patterns (PAMPs)," whereas the evolution of a less conserved or novel species-specific signatures that suppress host defense mechanisms are known as "effectors". Generally, effectors counterattack the PAMP-triggered immunity (PTI), which would get activated immediately after perception of the pathogen (Boller and Felix 2009). While most of the effectors are actively secreted, PAMPs are not typically actively secreted. On the other hand, without the real-time confrontation of the pathogen, the extraneous application of these PAMPs and certain effectors (based on host genotype) can induce host defense similar to resistance inducers/elicitors (Boyd et al. 2013; Anil et al. 2014). The active resistance, thus induced by the process of priming may be systemic, durable, and capable of acting against subsequent attacks of pathogens (Conrath et al. 2006, 2015). Hence, the strategy of employing effective resistance inducers and identification of new pathogen signatures, which can sensitize the host, either by enhancing or suppressing host defense would aid in disease management as well as deciphering disease resistance or suppression-associated genes, respectively.

Hithero, a multitude of host resistance-inducing secreted PAMPs/elicitors has been identified from a wide range of pathosystems, while a handful of secreted PAMPs have been functionally demonstrated to induce disease resistance upon priming (Walters et al. 2013; Burketova et al. 2015; Hamid and Wong 2017). For instance, priming with harpin, cerato-platanin, and elicitin class of PAMPs have been reported to enhance disease resistance by inducing the production of plethora of defense-related compounds. Further, overexpression of the PAMPs like harpins, flagellins, cerato-platanins, and elicitins has also been reported to enhance a broad spectrum of disease resistance against bacterial and fungal pathogens in model plants (Shao et al. 2008; Takakura et al. 2008; Yang et al. 2009; Du et al. 2015).

Priming of sugarcane with benzothiadiazole (BTH), an analogue of salicylic acid and Cf elicitor, a glycoprotein derived from the cell wall of *C. falcatum* has been shown to induce the production of various defense-related compounds and suppress red rot severity (Ramesh Sundar et al. 2008, 2009; Ashwin et al. 2017a). The application of these inducers has been reported to upregulate the expression of many defense-related transcription factors and resistance gene analogs (RGAs) (Muthiah et al. 2013; Selvaraj et al. 2014). However, the factors such as cost-effectiveness and the complexity in mass production of BTH and Cf elicitor, respectively, have restricted the employment of these inducers for large scale field applications. Recently, a study on comparative secretomic analysis of *C. falcatum* cultures that differed in virulence has identified CfEPL1 (eliciting plant response-like) protein, a potential PAMP that induces systemic resistance in sugarcane (Ashwin et al. 2017b). Besides, the study has identified few pathogenicity-related proteins and highlighted the importance of mining the secreted proteins of *C. falcatum*.

On the whole, the hurdles confronted with BTH and Cf elicitor combined with the significance of elucidating functional information of pathogen signatures have necessitated scouting for identification of defense triggering protein(s) from *C. falcatum* secretome. Therefore, in this study, we systematically screened the secretome of *C. falcatum* and identified a novel protein that possesses defense elicitation property. Besides, this study has also characterized the functional importance of putative domains of the identified novel protein through a series of bioassays in sugarcane and *Nicotiana tabacum.*

Materials and methods

Fungal culture and plant materials

A standard high virulent isolate of *C. falcatum*, *Cf*671 (Microbial Type Culture Collection and Gene Bank, Chandigarh, India, accession number 12142), was used for all the experiments in this study. It was cultured on oat meal agar plates and incubated at 28 °C with 14-:10-h light and dark cycles (light intensity 100 μmol/m^2/s) (Model MIR554, Panasonic Healthcare Co., Ltd., Gunma, Japan). The plates were subcultured once in every fortnight for maintenance of the culture. Eight-month-old sugarcane cultivars, namely,

CoC 671 (red rot susceptible) and Co 93009 (red rot resistant), grown under natural climatic conditions at the institutional experimental farm (ICAR—Sugarcane Breeding Institute, Coimbatore, India) were used in this study. For certain bioassays, 2-month-old greenhouse grown *N. tabacum* plants were used. To establish sugarcane cell suspension cultures, friable embryogenic calli generated from meristematic tissues of CoC 671 were used (Ramesh Sundar and Vidhyasekaran 2003).

Protein extraction, fractionation, and purification

For extraction of secreted proteins from *C. falcatum,* mycelial discs of around 5 mm diameter were inoculated in ten 500-mL flasks each containing 150 mL of oat meal broth and incubated at 28 °C for 10 days without agitation with similar light and dark cycles as stated above. After 10 days of incubation, the mycelial mats were harvested and the spent medium was clarified by centrifugation. The supernatant was then serially filtered through 0.8- and 0.45-μm membrane filters (Supor® PES, Pall Corporation, MI, USA) to ensure removal of spores, mycelial filaments, and particulates of oat meal broth, if any. To extract total secreted proteins from this filtrate in its native form, ammonium sulphate ($(NH_4)_2SO_4$) precipitation method was used as described by Ashwin et al. (2017b). Briefly, ($(NH_4)_2SO_4$) salt was slowly added to the filtered spent medium, until it reaches a 90% saturation at 4 °C, while constantly mixing with a magnetic stirrer for 20 h. Precipitated proteins were then recovered using centrifugation at 12,000 rpm for 30 min and resuspended in a buffer (Buffer A) that composed of 10 mM tris, 40 mM sodium chloride (NaCl), 1 mM dithiothreitol, and 10% glycerol with a pH of 7.5. In order to desalt the residual $(NH_4)_2SO_4$ from the protein solution, they were washed with 20 volumes of buffer A using 10 kDa Amicon ultra-15 centrifugal ultrafilters (Merck Millipore, County Cork, Ireland).

To fractionate the total secreted proteins based on size, ultrafilters with different cutoff ranges were used. First, the desalted protein solution was filtered using 50-kDa Amicon ultra-15 centrifugal ultrafilters (Merck Millipore, County Cork, Ireland). While the retentate containing proteins greater than 50 kDa was collected and marked as > 50 kDa fraction, the filtrate was subjected to further fractionation with a 30-kDa filter. The resultant retentate representing the proteins ranging from 30 to 50 kDa was marked as 30–50 kDa fraction, and the remaining filtrate was just concentrated and marked as 10–30 kDa fraction. Besides these three fractions, total secreted proteins from the filtered spent medium were directly fractionated by sequential precipitation with different saturation levels of ($(NH_4)_2SO_4$), namely, 0–30, 30–60, and 60–90% (Dixon and Webb 1962; Wingfield 2016). These protein fractions were immediately desalted with buffer A as described above and used for bioassay-based screenings.

Anion exchange chromatography (AEC) using Bio-scale mini macro-prep high Q cartridge (Catalog no. 732-4122, Bio-Rad Laboratories, Inc., CA, USA) was employed for further separation of active protein fraction in BioLogic™ LP liquid chromatography system (Bio-Rad, Laboratories, Inc., CA, USA). Here, the proteins were eluted with a linear gradient of 0.04 to 1 M NaCl in the same buffer. Based on the chromatogram, individual tubes corresponding to a single peak were pooled and marked as a single fraction. Prior to bioassay, these pooled peak-specific fractions were desalted and concentrated as described above. The active protein fraction was further purified by size exclusion chromatography (SEC) by employing Agilent Bio SEC 5 μm, 150 Å column in Agilent 1260 infinity HPLC system (Agilent Technologies Inc., Waldbronn, Germany). At each stage and whenever required, protein concentrations were quantified by Bradford method, using BSA as reference standards. Similarly, the quality of the extracted and fractionated proteins was ascertained with 1-DE (SDS-PAGE).

Bioassays on sugarcane suspension culture

After elicitation with fractionated or purified proteins, changes in the extracellular pH of CoC 671 suspension cells were monitored at different time intervals until 3 h post-elicitation. Similarly, the accumulation of hydrogen peroxide (H_2O_2) was quantified at different time intervals as described by Bindschedler et al. (2001). In brief, 300 μL of suspension cells was drawn at different time points and centrifuged at 12,000 rpm for 15 s. Then, 100 μL of supernatant was immediately added to 1 mL of freshly prepared xylenol orange reagent and incubated at room temperature for 30 min. After incubation, the absorbance of the mixture was measured at 560 nm. Absorbance values of the test samples were then plotted against the standards prepared with different concentrations of H_2O_2. BTH, a well demonstrated resistance-inducing agent in sugarcane, was used as a positive control for studying defense elicitation. The level of H_2O_2 accumulation was detected at 48 h post-elicitation by using DAB staining method as described by Ashwin et al. (2017b). For DAB staining, 10 μL/mL of 3,3′-diaminobenzidine (DAB) tetrahydrochloride hydrate (Sigma-Aldrich Co. LLC, MO, USA) (1 mg/mL) solution, pH 3.8, was added immediately after the elicitation of suspension cells with fractionated or purified proteins and incubated under dark conditions for 48 h. The development of the brown precipitate, as a result of reaction between DAB and H_2O_2, was documented both macroscopically and microscopically. For all DAB staining assays, ascorbic acid, the quenching agent of H_2O_2, was separately amended with their respective positive control to verify whether the browning of the cells was exclusively due to H_2O_2 production.

For certain experiments, viability of suspension cells was determined using Evans blue as described by Davies et al.

(2006). After 48 h of elicitation, 0.05% (*w*/*v*) of Evans blue was added with 1 mL of suspension cells and incubated for 15 min at room temperature. Unbound dye was removed by extensive washing of the cells with Milli-Q grade water and the dye that was bound to the dead cells was solubilized by grinding them in 50% methanol containing 1% SDS and incubating the homogenate at 50 °C for 30 min. After incubation, the absorbance of the supernatant was measured at 600 nm. Percentage of cell death was calculated by considering the relative absorbance values of heat-treated cells as 100% death and the mock-treated cells as 0% death. Three replications were used for all these bioassays, whereas only the representative images were presented for DAB staining.

Bioassays on *N. tabacum*

To evaluate the defense elicitation properties of fractionated or purified proteins on a nonhost model system, 50 μL of protein solutions was infiltrated on the adaxial side of *N. tabacum* leaves using a needleless syringe. After 24 and 48 h of infiltration, the spots were macroscopically examined for the development of hypersensitive responses (HR), if any. To detect the level of H_2O_2 accumulation in response to perception of proteins, the infiltrated portion of the leaves was excised (3 cm in diameter) and stained with DAB as described by Chen et al. (2012). In brief, after 24 h of infiltration, the leaf discs were excised and stained with DAB solution (1 mg/mL) at room temperature for 8 h under dark condition. Stained discs were then bleached in 95% ethanol for 20 min and mounted in 50% glycerol for observation under light microscope. Meanwhile, to detect callose deposition, the leaf discs were completely cleared with ethanol-acetic acid (3:1, *v*/*v*) solution for 24 h, followed by a wash with 50% ethanol and three consecutive washes with 70 mM dipotassium hydrogen phosphate buffer (pH 9). The discs were then stained with 0.05% aniline blue prepared in 70 mM dipotassium hydrogen phosphate buffer (pH 9) for 2 h. After a brief rinsing with distilled water, the discs were mounted in 50% glycerol and observed under UV illumination using an epifluorescence microscope. Each of these experiments was repeated three times and only the representative images were presented here.

MS/MS analysis and database search

The purified active protein fraction was electrophoresed (SDS-PAGE) on a 20-cm-long gel in Ettan DALT six electrophoresis unit (GE Healthcare Bio-Sciences AB, Uppsala, Sweden) and the band that represented a single protein was manually excised and subjected to MALDI TOF/TOF analysis as described by Barnabas et al. (2016). After destaining, the spot was alternatively washed with 50 mM ammonium bicarbonate (NH_4HCO_3) and 50% acetonitrile for four times and subjected to in-gel digestion with sequencing-grade modified trypsin (Promega Corporation, Madison, USA) for 12 h. Digested peptides were then extracted with 50% acetonitrile containing 0.1% trifluoroacetic acid (TFA). For MALDI TOF/TOF analysis, equal volumes of digested peptides and α-cyano-4-hydroxycinnamic acid (CHCA) solution (5 mg/mL of CHCA in 70% acetonitrile with TFA 0.1%) were mixed and spotted in triplicates onto a standard 386-well stainless steel MALDI target plate in 4800 Plus MALDI TOF/TOF Analyzer (AB Sciex, CA, USA) and the spectra were collected in a data dependent mode. After a survey scan (MS), MS/MS was performed for the 10 most abundant ions and all the spectra were exported for post-MS analysis.

For protein identification, the above-obtained MS/MS spectra were searched against two different *C. falcatum*-specific protein databases, viz., transcriptome shotgun assembly (Bioproject PRJNA272832) (Prasanth et al. 2017) and whole genome shotgun assembly (Bioproject PRJNA272959) of *Cf*671 isolate using Peaks studio software (Version 8; Bioinformatics Solution Inc., ON, Canada), which was supported with de novo, Peaks DB, PTM, and Spider algorithms. The set search parameters were 1+ for peptide charge state, 50 ppm for peptide mass tolerance, 0.3 Da for fragment mass tolerance, and 1 and 3 for maximum allowed missed cleavage and PTM predictions, respectively. Besides, carbamidomethylation (C) and oxidation (M) were set for fixed and variable modifications, respectively. Average local confidence and −10lgP threshold for fetching peptide spectral matches (PSMs) were set to ≥ 50, to eliminate false positive identifications. False discovery rate (FDR) of PSMs was also estimated by decoy fusion method during Peaks DB search.

In silico analysis

The identified protein was annotated using BLASTP search and the parameters like theoretical molecular weight and pI were predicted using ProtParam tool (ExPASy, Swiss Institute of Bioinformatics). Multiple sequence alignment was performed with Clustal Omega (http://www.ebi.ac.uk/Tools/msa/clustalo/). For validation of secretory nature of the protein and signal peptide domain prediction, SignalP v 4.1(www.cbs.dtu.dk/services/SignalP/) and TargetP v 1.1 (www.cbs.dtu.dk/services/TargetP/) were used. Besides, the probability of being an effector or possessing effector properties was predicted using EffectorP v 1.0 (http://effectorp.csiro.au/) (Sperschneider et al. 2016).

Cloning, expression, and purification

For functional characterization, different domain deletional variants of the purified protein sequences were constructed in pET28a expression vector (Novagen® Merck Millipore, Darmstadt, Germany) with 6X His and T7 fusion tags at N-terminal end and expressed in the *Escherichia coli* strain

Rosetta™ 2(DE3)pLysS (Novagen® Merck Millipore, Darmstadt, Germany). Briefly, the truncated sequences of the gene that encode the purified protein were amplified with restriction site linked sequence-specific primers (Table S1a in the supplementary material). These inserts and pET28a vector were separately double digested with *Eco*RI and *Sal*I (ThermoFisher Scientific Inc., Waltham, USA) and ligated with T4 DNA Ligase (ThermoFisher Scientific Inc., Waltham, USA). After ligation, they were transformed into Rosetta™ 2(DE3)pLysS cells and grown on kanamycin-containing Luria Bertani (LB) agar plates. The veracity of the positive clones was verified by colony PCR, restriction digestion, and Sanger sequencing. To express the protein of interest, these positive transformants were allowed to grow up to 0.5 OD and induced with 0.5 mM isopropyl β-D-1-thio-galactopyranoside (IPTG) at 30 °C for 4 h. After which, the cells were pelleted down by centrifugation at 6000 rpm for 5 min and resuspended in 0.1 volume of extraction buffer (50 mM Tris, 200 mM NaCl, 10 mM β-mercaptoethanol, 10% glycerol). The suspension was then subjected to three cycles of freeze-thaw shocks and briefly sonicated at 10 s pulse on, 10 s pulse off for 1 min at 30% amplitude for cell lysis. The lysates were then centrifuged at 13,000 rpm for 10 min at 4 °C and the supernatant that contained the recombinant proteins was purified using a Ni-Sepharose 6 Fast Flow column (GE Healthcare Bio-Sciences, AB, Uppsala, USA), a low pressure chromatography system (BioLogic™ LP System, Bio-Rad, Laboratories, Inc., CA, USA). Here, the recombinant his-tag proteins were eluted against a linear gradient of extraction buffer containing 500 mM imidazole from 0 to 500 mM for 30 min. Fractions containing recombinant proteins were immediately desalted with buffer A as described above and purified further by size exclusion chromatography using Sephacryl S100 HR column.

Western blot

The purity of recombinant proteins was verified by immunoblotting using T7 tag-specific antibody as described by Ashwin et al. (2017b). In brief, purified proteins were electrophoresed and transferred into an activated polyvinylidene fluoride (PVDF) membrane (0.2 μm) by semi-dry transfer method using Trans-Blot® SD Semi-Dry Transfer Cell (Bio-Rad, Laboratories, Inc., CA, USA). After blocking, the membrane was incubated with T7 tag-specific primary antibody (T7 Tag Monoclonal antibody, Merck Millipore, USA) followed by the secondary antibody (Goat Anti-Mouse IgG-Alkaline Phosphatase antibody, Sigma-Aldrich Co. LLC, MO, USA) and developed with the substrate 5-bromo-4-chloro-3-indolyl phosphate (BCIP) in conjunction with Nitro blue tetrazolium (NBT). For priming and bioassays, fusion tags of purified recombinant proteins were removed using Thrombin CleanCleave™ Kit (Sigma-Aldrich, Co. LLC, MO, USA) by centrifugation recovery method as per manufacturer's instructions.

Defense priming and detached leaf bioassays

To evaluate the priming efficacy of recombinant proteins, 8-month-old CoC 671 canes were foliar sprayed (25 mL/cane) twice with optimum concentration of recombinant proteins at 10-day interval using a handheld sprayer. After 2 weeks, primed and unprimed (mock-treated) canes were inoculated with *Cf*671 spore suspension by nodal swabbing method as described by Viswanathan et al. (1998). In brief, the leaf sheaths around the sixth node (from the meristematic cane top) were removed and the pathogen was inoculated by wrapping a thin wad of absorbent cotton, which was drenched with 2 mL of spore suspension (10^6 spores/mL). In order to maintain the moisture to facilitate germination and penetration of the pathogen into the root primordia and leaf scar, the inoculated nodal portion was completely covered with Parafilm® "M" film (Sigma-Aldrich, Co. LLC, MO, USA). For pathogen quantitation and gene expression analysis, the stalk samples of primed and unprimed canes were collected at different time points (0, 12, 24, 48, 72, 120, and 600 h post-inoculation (hpi)) and stored at − 80 °C until further processing.

On the other hand, after 2 weeks of foliar spray, matured third leaves of primed and unprimed canes were detached and subjected to detached leaf bioassay as described by Ashwin et al. (2017b). Briefly, the bottom portion of the detached leaves was excised and washed and minor injuries (few pin-pricks in approximately 5 mm^2 area) were made in the lamina on both sides of the midrib to breach the thick cuticle layer enriched with waxes. After that, 50 μL of *Cf*671 spores (10^6 spores/mL) was inoculated on the injured surface and incubated in an illuminated chamber (Model E41L2, Percival Scientific Inc., IA, USA) maintained at 28 °C with 60% humidity and 14:10 h light-dark cycling conditions. For co-infiltration experiment, *Cf*671 spore suspension (10^6 spores/mL) was prepared in the recombinant protein solution and inoculated on unprimed detached leaves as described above. After 72 h, the leaves were assessed both macroscopically and microscopically for lesion development and infection structures, respectively. While the brownish yellow lesion length was measured using a ruler, the number of appressorium per square millimeter area was counted from 10 different spots (250 μm^2) per leaf to minimize errors. Each set of treatments comprised of five independent replications and the experiment was repeated three times for reproducibility.

Statistical analysis

Quantitative datasets representing lesion length and number of appressorium were subjected to Kolmogorov-Smirnov test, Shapiro-Wilk's test, and Levene's test to check the

assumptions of normality and homogeneity of variance. They were then statistically analyzed using one-way analysis of variance (ANOVA). The differences between the treatments were analyzed by post hoc Tukey's test at the significance of $p \leq 0.05$ using the software IBM SPSS statistics 21.0 (SPSS, Chicago, USA).

C. falcatum biomass quantitation and gene expression analyses

For in planta pathogen biomass quantitation, genomic DNA from the nodal portion (covering approximately 2 cm above and below the site of pathogen challenge) of the stalk samples collected at different time points (0, 12, 24, 48, 72, 120, and 600 hpi) were extracted using CTAB method. The biomass of *C. falcatum* was then quantified using the constitutively expressing gene, eukaryotic elongation factor (*CfeEF1α*) by absolute quantification method using qPCR (Diguta et al. 2010). A standard curve was generated from *CfeEF1α* amplification from tenfold dilutions of *C. falcatum* DNA with a linear relationship (R^2 value) of 0.989. Quantitation cycle (Cq) values of the test samples were then substituted in the standard curve equation to determine the quantity of pathogen biomass.

For gene expression analyses, total RNA was extracted from the nodal region as described above using TRI Reagent® (Sigma-Aldrich Co. LLC, MO, USA) and then converted into cDNA using RevertAid™ H minus First Strand cDNA Synthesis Kit (ThermoFisher Scientific, Waltham, USA). Among the constitutive genes of sugarcane, viz., *ScEF1α*, *ScGAPDH*, and *Sc25S rRNA*, the elongation factor *ScEF1α* was found to be the most stable reference gene by the tool NormFinder Excel add-in v 0.953 (https://moma.dk/normfinder-software) for qRT-PCR analysis. Similarly, *C. falcatum* elongation factor (*CfeEF1α*) was found to be the most stable reference gene, among *CfeEF1α* and Cf actin genes. Therefore, the expression of target genes from sugarcane and *C. falcatum* was normalized with the expression of *ScEF1α* and *CfeEF1α*, respectively. Three biological replicates with two technical duplicates each were used for all qPCR analyses. All these analyses were performed in StepOnePlus™ Real-Time PCR (Applied Biosystems, CA, USA) using Power SYBR Green PCR Master Mix (Applied Biosystems, CA, USA). The details of primer sequences, amplicon length, amplification efficiency, and annealing temperature were listed (Table S1b in the supplementary material). Melt curve analysis was also performed to verify the amplification specificity of target genes. Relative fold expression and respective standard deviation of target genes were determined by $2^{-\Delta\Delta C_T}$ method.

The nucleic acid sequences of all the genetic products like full length genes, truncated genes, and the genes employed for expression analyses were submitted in GenBank and their respective accession numbers were listed in Table S1 in the supplementary material.

Results

Fractionation and bioassays for screening of elicitor-active protein fraction(s)

To identify a *C. falcatum* protein that could induce or trigger host defense mechanism, a systematic top-down approach was adopted as described in the schematic diagram (Fig. S1 in the supplementary material). Initially, the extracted secreted proteins were fractionated with different saturation levels of $(NH_4)_2SO_4$ (0–30, 30–60, and 60–90%) and different cutoff ranges of centrifugal ultrafilters (10–30, 30–50, and > 50 kDa) for step by step screening of elicitor-active protein containing fraction(s). Fractionation quality of all these six fractions was subsequently verified by SDS-PAGE (Fig. 1).

As part of the preliminary screening of elicitor-active fraction(s), these six fractions were subjected to a series of bioassays that include quantification and detection of H_2O_2, the primary messenger of plant defense in sugarcane suspension cells, and observation for the development of HR in *N. tabacum*. After elicitation of CoC 671 suspension cells with fractionated proteins (250 μg/mL), the level of H_2O_2 was quantified at different time points. Among the six fractions, a steep increase in H_2O_2 production was observed with 10–30 kDa and 60–90% $(NH_4)_2SO_4$ fractions at 30 min post-elicitation, which gradually reduced to reach a plateau after 120 min (Fig. 2a). However, the 30–60% $(NH_4)_2SO_4$ fraction elicited only half of the level of H_2O_2 elicited by the above two fractions. In contrast, the 30–50 kDa, > 50 kDa, and 0–30% fractions elicited the least quantity of H_2O_2 at 30 min and attained the basal level of mock control after 120 min.

When the same batch of suspension cells was stained with DAB at 48 h post-elicitation, similar patterns of H_2O_2 accumulation level were observed visually (Fig. 2b). When the protein fractions (250 μg/mL) were infiltrated on *N. tabacum* leaves (a standard experiment to establish defense elicitation properties), only 10–30 kDa, 30–60%, and 60–90% $(NH_4)_2SO_4$ fractions triggered rapid HR development (Fig. 2c), which were in line with the results of H_2O_2 assays. A critical observation of SDS-PAGE profiles of these three fractions (10–30 kDa, 30–60%, and 60–90%) revealed a similarity in protein banding pattern in the range of 10–25 kDa. Therefore, the 10–30-kDa fraction that had the least number of total proteins while representing the common proteins (10–25 kDa range) among the three was selected for further fractionation and screening. Since the results of HR assays in the tobacco leaves were correlated with the results of H_2O_2 assays in sugarcane suspension cells, only HR assay was employed

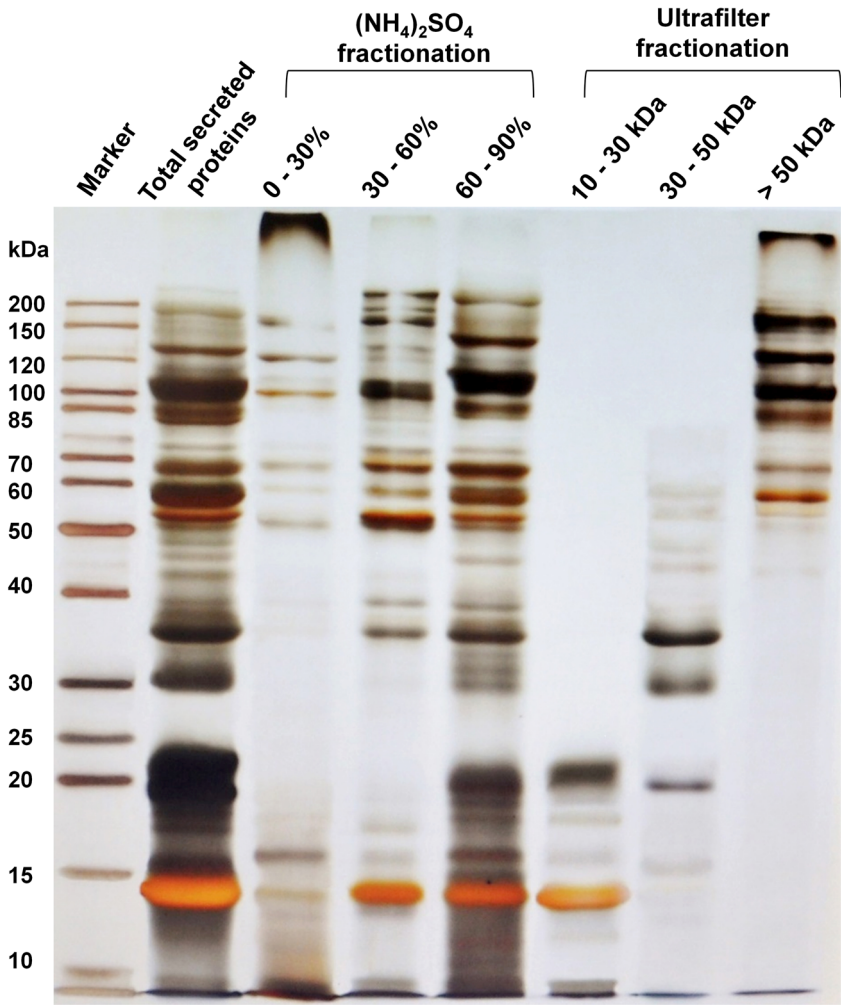

Fig. 1 Fractionation of secreted proteins of in vitro cultured *C. falcatum* using ammonium sulphate ($(NH_4)_2SO_4$) precipitation and size-based ultrafilters

for further screening of elicitor-active protein containing fractions.

Anion exchange chromatography-based separation of the elicitor-active 10–30-kDa ultrafilter fraction resulted in six major peaks (Fig. 3a). The fractions representing these peaks (I, II, III, IV, V, and VI) were separately collected, desalted, and analyzed through SDS-PAGE (Fig. 3b). HR assay of these fractions showed that the fractions "IV" and "V" have triggered HR development (Fig. 3c). However, the extent of HR triggered by fraction "V" was relatively far higher than fraction "IV" and equal to the 10–30-kDa fraction in all three replications. Therefore, the fraction "V" that contained two prominent protein bands was selected for further separation and purification using size exclusion chromatography. The HPLC chromatogram profile of this size-based separation vis-a-vis purification showed two distinct prominent peaks (Fig. 4a). The purity of this separated protein was subsequently verified by SDS-PAGE (Fig. 4b). Evaluation of these two purified proteins on *N. tabacum* leaves revealed that the protein represented by fraction "I" was responsible for the development of HR (Fig. 4c). Altogether, this systematic molecular sieving process has led to the discovery of an approximately 14-kDa secreted protein that induced defense responses in sugarcane and triggered HR in *N. tabacum*.

MS/MS-based identification and in silico analysis of the HR-inducing protein

To identify the HR-inducing protein, the protein spot was subjected to MALDI TOF/TOF MS and the collected spectra were searched against *C. falcatum Cf*671-specific databases using Peaks 8 studio tool. The search resulted in a unanimous hit of a hypothetical protein with 10 PSMs that had a coverage of 58% and FDR of ≥ 0.0% (Table S2 in the supplementary material). An attempt to annotate this full length hypothetical protein (132 amino acids) using protein BLAST revealed that this protein was novel with not more than 40% similarity with other proteins (Fig. S2a in the supplementary material). The search has indicated that this novel protein was recently identified as one of the high abundant proteins expressed by the virulent light-cultured *C. falcatum* and provisionally named as second hypothetical protein (HYP2) by our group (Ashwin

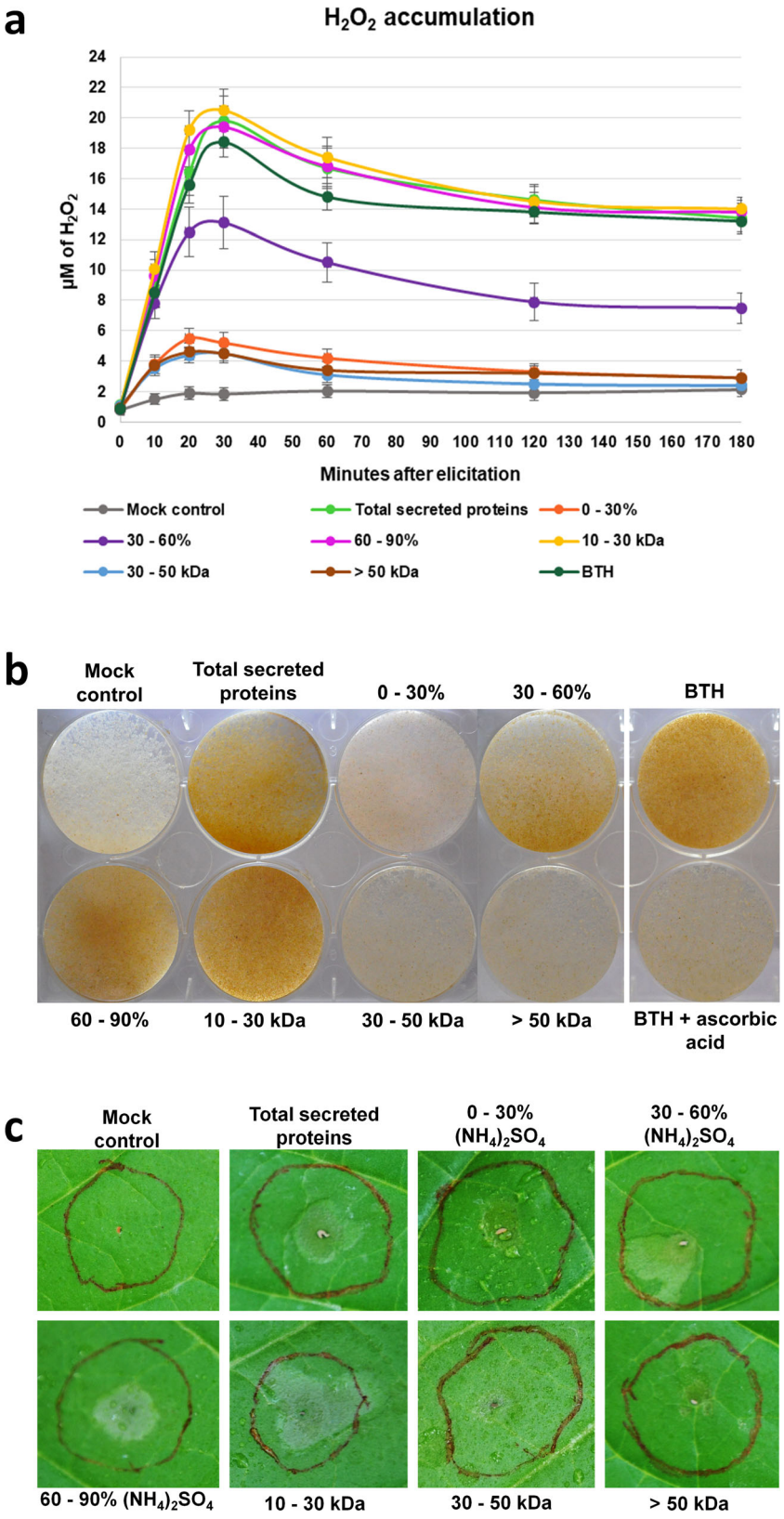

Fig. 2 Preliminary screening of $(NH_4)_2SO_4$ and ultrafilter fractions of secreted proteins using a series of bioassays. **a** Temporal accumulation profile of H_2O_2 in sugarcane cv. CoC 671 suspension cells after elicitation with fractionated proteins. **b** Detection of H_2O_2 production in DAB spiked sugarcane cv. CoC 671 suspension cells at 48 h after elicitation with fractionated proteins. **c** Screening of fractionated proteins for HR induction in *Nicotiana tabacum* leaves at 24 h post-infiltration. BTH was used as a positive control to estimate and detect H_2O_2 levels in **a** and **b**, respectively. Zero to 30, 30–60, and 60–90% represent the fractions of $(NH_4)_2SO_4$ precipitation, whereas 10–30, 30–50, and > 50 kDa represent the fractions of size-based ultrafiltration. For mock control, assay buffer (buffer A) was used

et al. 2017b). Notably, the next closest hits of this protein were irregularly distributed in all three major divisions of the fungal kingdom, viz., Ascomycota, Basidiomycota, and Mucoromycota (Fig. S2b in the supplementary material).

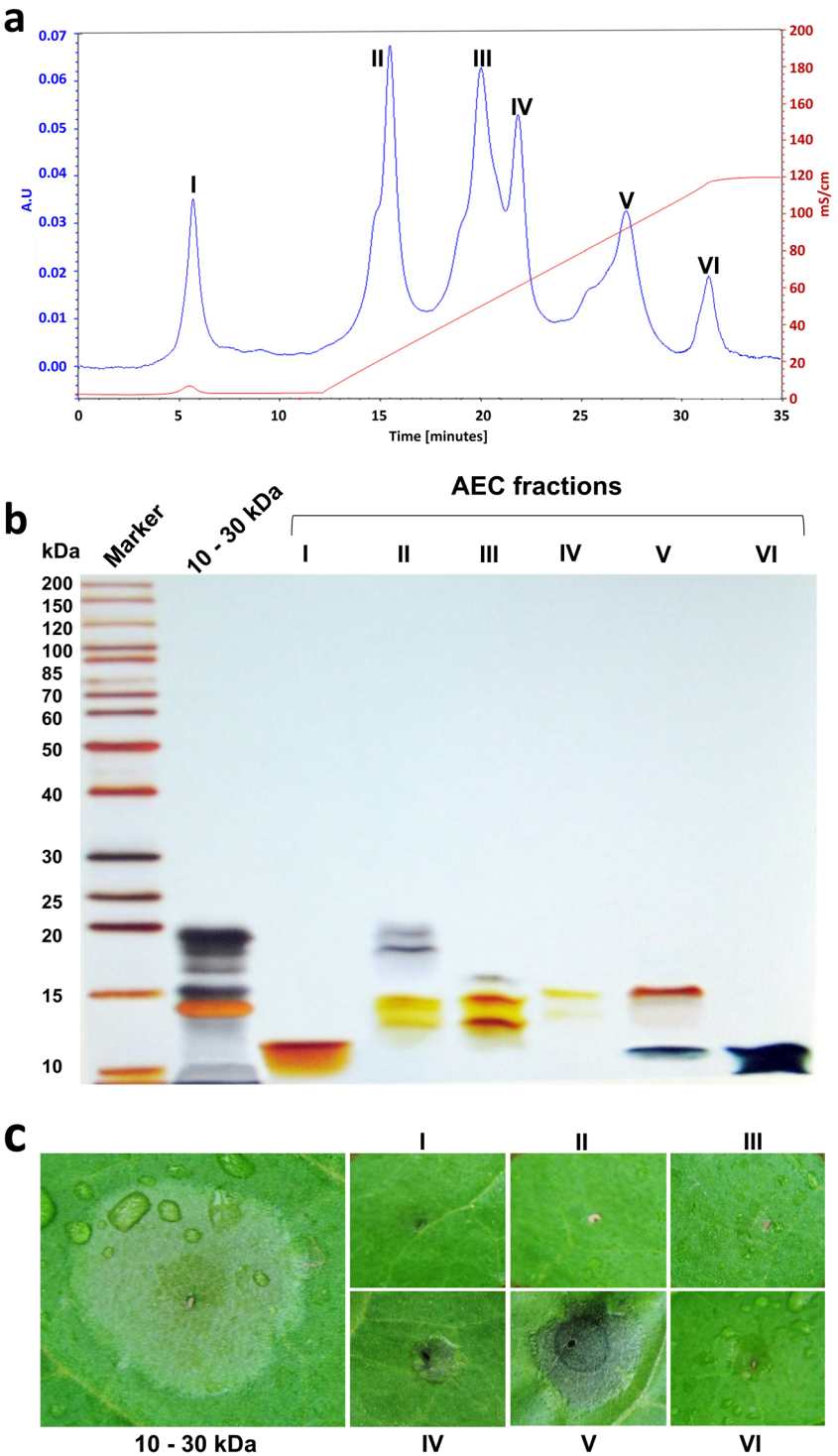

Fig. 3 Separation of 10–30 kDa ultrafilter fraction by anion exchange chromatography (AEC) and subsequent screening for HR induction. **a** Separation of 10–30 kDa ultrafilter fraction containing proteins by AEC using Bio-Scale Mini Macro-Prep High Q Cartridge (Bio-Rad, Laboratories, Inc., California, USA). **b** SDS-PAGE profile of desalted AEC fractions. **c** Screening of AEC fractions for HR induction in *N. tabacum* leaves at 24 h post-infiltration

Multiple sequence alignment of few closest hits has indicated that this novel protein contains a novel motif of conserved pattern of six cysteine residues (Fig. S2c in the supplementary material), which suggest that this protein could belong to a novel family of small secreted proteins (SSPs). Owing to this novelty and its functional properties, henceforth, we designate this protein as *C. falcatum* plant defense-inducing protein 1 (CfPDIP1). Further, gene isolation and analysis indicated that the genomic DNA sequence (NCBI accession code KY178273.1) of this *CfPDIP1* gene contains a 5′ untranslated region (1–12 bases) and one single intron of 178 bp size, which starts from 235th and the 412th base position (Fig. S3a in the supplementary material).

Signal peptide analysis of the identified CfPDIP1 protein with SignalP and TargetP tools confirmed its secretory nature and predicted the presence of a signal peptide

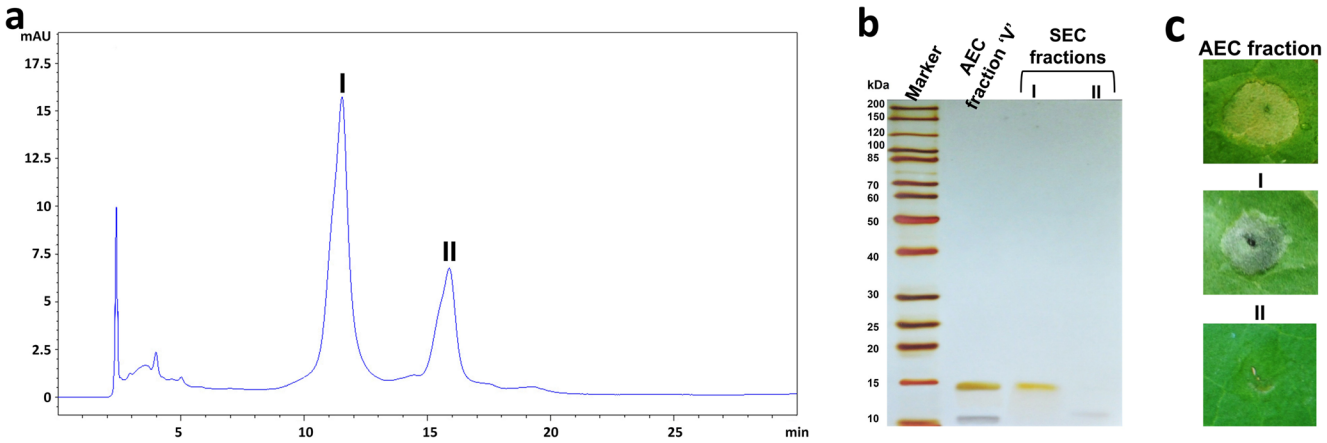

Fig. 4 Purification of HR-inducing protein from AEC fraction "V" by size exclusion chromatography (SEC) and subsequent screening for HR induction. **a** Purification of HR-inducing protein from the elicitor-active AEC fraction "V" by SEC using Agilent Bio SEC-5 µm, 150 Å column. **b** SDS-PAGE profile of SEC fractions. **c** Identification of HR-inducing protein fraction through HR assay on *N. tabacum* leaves at 24 h post-infiltration

with the cleavage site between 21st and 22nd residues in the N-terminal region (Figs. S3b and S3c in the supplementary material). The graphical representation of PSM coverage on full length CfPDIP1 hit, as shown by Peaks 8 studio tool, also indicated that they were devoid of this predicted signal peptide region (Fig. 5a). Since the CfPDIP1 protein was identified as one of the high abundant proteins expressed by the virulent *C. falcatum* pathotype by Ashwin et al. (2017b), the CfPDIP1 protein sequences with and without signal peptide were analyzed

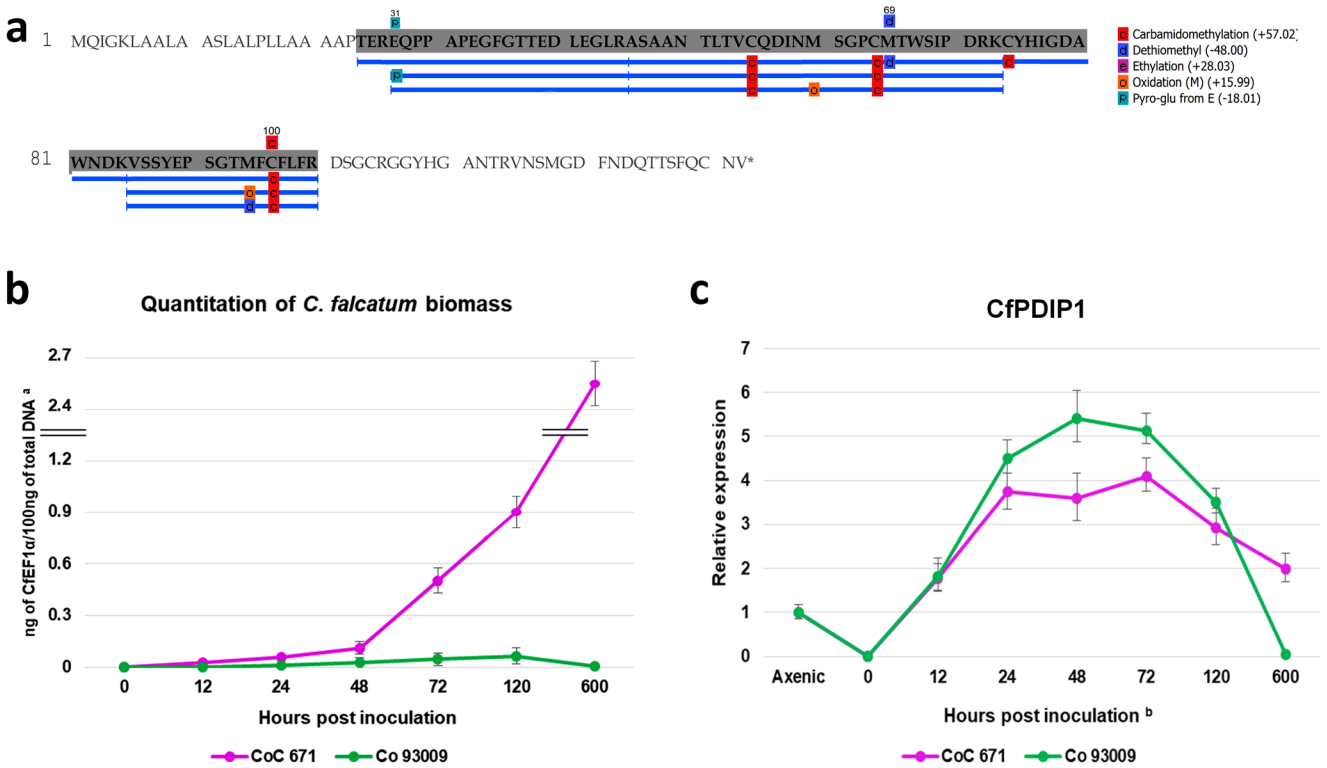

Fig. 5 PSM coverage of the identified HR-inducing protein (CfPDIP1) and expression profiling of *CfPDIP1* transcript during compatible and incompatible interaction with the sugarcane cultivars CoC 671 and Co 93009, respectively. **a** PSM coverage of the HR-inducing protein identified by MALDI TOF/TOF MS using Peaks studio 8.0 tool along with the prediction of fixed, variable, and other post-translational modifications. **b** Temporal quantification of in planta biomass of *C. falcatum* by absolute quantification method. Superscript a: *Y*-axis values were broken (vertical bars) to make the small increments in pathogen biomass of Co 93009 is visible. **c** Temporal expression pattern of *CfPDIP1* transcript by comparative C_T method. Superscript b: Numerical values in *X*-axis indicate hours post-inoculation except the in vitro axenic culture of *C. falcatum*. "0 h" indicates mock inoculated control. Error bars indicate standard deviation of three biological replicates with two technical replicates each

with EffectorP tool (Table S3 in the supplementary material). This analysis predicted that both forms of CfPDIP1 proteins could possibly act as effectors during host-pathogen interactions. Altogether, these in silico analyses substantiated the MS-based identification of the HR-inducing protein as novel CfPDIP1 protein and its theoretical properties were found to be corroborated with the observed attributes.

Transcriptional profiling of CfPDIP1 expression during compatible and incompatible interactions

CfPDIP1 protein, by virtue of its potential in triggering host defense responses and its predicted effector role, the transcriptional abundance of *CfPDIP1*, was profiled in planta at different time points during compatible and incompatible interactions with sugarcane. CoC 671 (red rot susceptible) and Co 93009 (red rot resistant) sugarcane cultivars were used to study compatible and incompatible interactions, respectively. Profiling of in planta pathogen biomass showed that the rate of pathogen colonization was relatively far higher in the compatible interaction than the incompatible one (Fig. 5b). Specifically, a distinct elevation in the rate of pathogen colonization was observed since 48 hpi in the compatible interaction. In contrast, in incompatible interaction, the colonization rate was restricted with a relatively far less quantity of pathogen biomass, which was completely vanished at 600 hpi (25 days post-inoculation). Relative expression profiling of *CfPDIP1* with respect to pathogen biomass showed that the expression of *CfPDIP1* was increased few fold in the incompatible interaction as compared to the compatible interaction between 24 and 72 hpi (Fig. 5c). However, in compatible interaction, the expression level was relatively less but observed throughout the period of colonization. Therefore, the significant differences in the expression level of *CfPDIP1* at the early stage of colonization during compatible and incompatible interactions necessitated an in-depth functional characterization.

Putative domain-based dissection and production of recombinant CfPDIP1 proteins

To characterize the functional properties of the novel CfPDIP1 protein, the full length CfPDIP1 protein sequence was putatively dissected into three distinct domains based on the signal peptide and the recently identified truncated isoform of this protein (Ashwin et al. 2017b) (Fig. 6a). Different sets of primers were designed to amplify and clone three different domain deletional variants of *CfPDIP1* in the pET28a expression vector, which resulted in the expression of 6X His and T7 fusion tags at the N-terminal end of the target proteins (Fig. 6b). These three domain deletional variants represented full length CfPDIP1 with signal peptide domain (CfPDIP1FL), full length CfPDIP1 without signal peptide domain (CfPDIP1ΔN1-21), and a truncated CfPDIP1 that putatively represents the isoform or the main domain (CfPDIP1ΔN1-45). Interestingly, in addition to the first two variants, the third variant, CfPDIP1ΔN1-45, was also predicted to possess the properties of an effector by EffectorP tool (Table S3 in the supplementary material).

SDS-PAGE analysis of these purified recombinant proteins showed more than one band, in addition to the expected molecular weight range in CfPDIP1ΔN1-21 and CfPDIP1ΔN1-45 fractions (Fig. 6c). Therefore, the purity of these recombinant proteins was assessed by western blot with T7 tag-specific antibody. The blotting profile revealed that the nonspecific bands observed in the purified CfPDIP1ΔN1-21 and CfPDIP1ΔN1-45 fractions were their respective dimeric and tetrameric forms. Interestingly, the recombinant CfPDIP1FL protein that had the signal peptide at the N-terminal end did not form any dimeric or tetrameric forms as evidenced in the sensitive western blot experiment.

Dose optimization of recombinant CfPDIP1 proteins for bioassays and defense priming

To determine the optimum concentration of recombinant CfPDIP1 proteins for bioassays and priming efficacy evaluations, CoC 671 suspension cells were treated with different concentrations of purified native CfPDIP1 protein and the parameters such as H_2O_2 accumulation and the concomitant relative percentage of cell viability were measured at 48 h post-treatment (Fig. S4 in the supplementary material). Results indicated that H_2O_2 induction was inversely correlated with the relative percentage of cell viability. Hence, 50 μg/mL, the minimum CfPDIP1 concentration that induced higher amount of H_2O_2 production (on an average of 15 μM H_2O_2) with minimal reduction of cell viability (< 20%), was considered as the optimum dosage concentration and used accordingly for subsequent experiments on functional characterization of recombinant CfPDIP1 proteins.

Functional characterization of recombinant domain deletional variants of CfPDIP1

To ascertain the functional role of CfPDIP1 and to characterize the significance of different domains of CfPDIP1, the recombinant domain deletional variants of CfPDIP1 proteins were subjected to various bioassays using CoC 671 suspension cells and *N. tabacum* leaves. The purified recombinant CfEPL1ΔN1-92 protein, a PAMP of *C. falcatum* which was

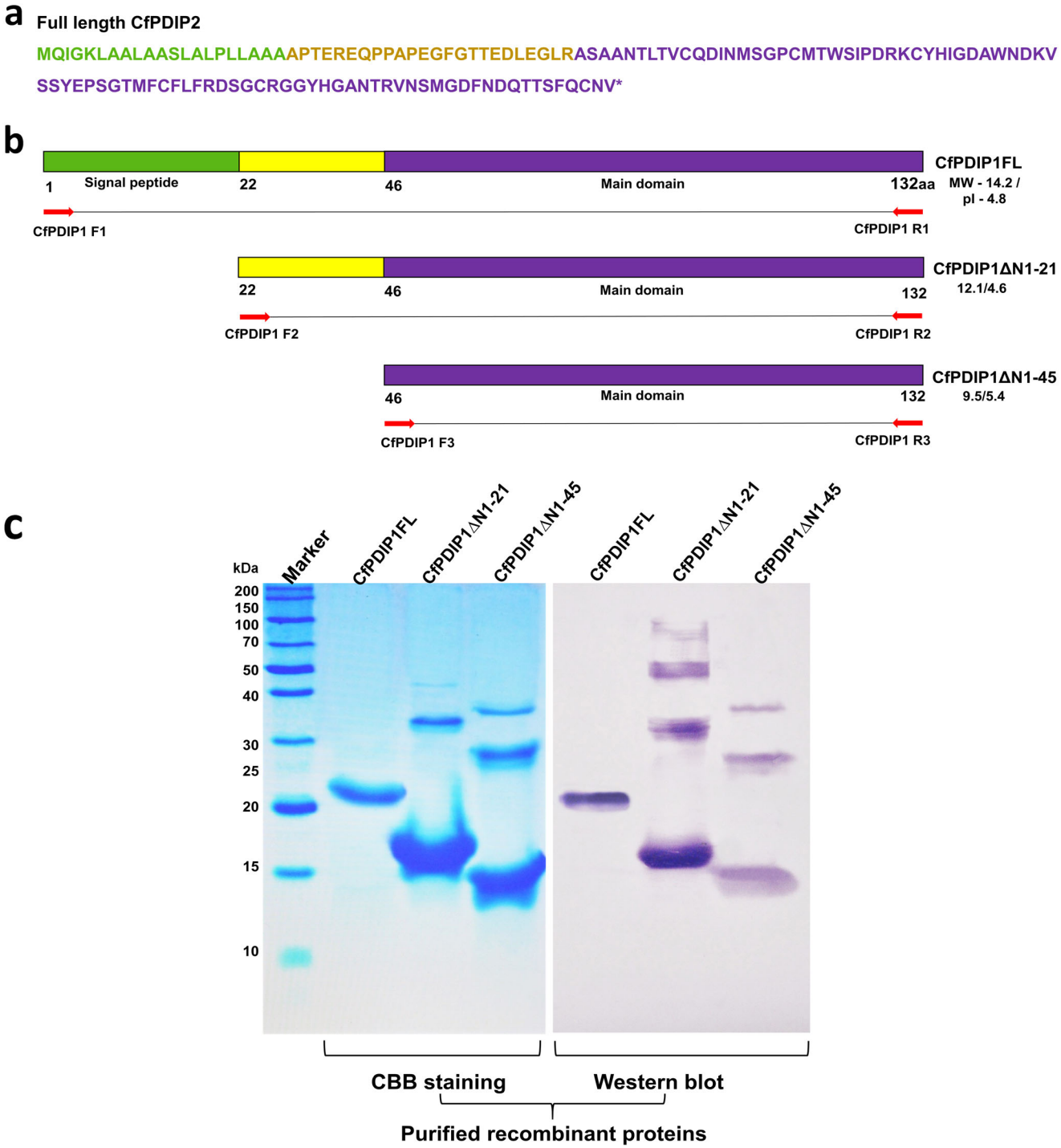

Fig. 6 Putative domain-based dissection, in vitro expression and purification of CfPDIP1 protein for functional characterization. **a** Full length protein sequence of CfPDIP1. Residues in different colors indicate putatively distinct domains. **b** Dissection of CfPDIP1 protein to generate different domain deletional constructs for in vitro expression and subsequent functional characterization. Lines begin and end with red arrows indicate the respective set of primers used for amplifying distinct constructs of CfPDIP1. **c** SDS-PAGE profiles of in vitro expressed and purified recombinant CfPDIP1 proteins observed under Coomassie brilliant blue (CBB) staining and western blotting with T7 tag-specific antibody (Merck Millipore). Except the full length CfPDIP1 protein (CfPDIP1FL), domain deletional recombinant CfPDIP1 proteins, viz., CfPDIP1ΔN1-21 and CfPDIP1ΔN1-45, exhibit dimeric and tetrameric forms

demonstrated to induce systemic resistance in sugarcane by Ashwin et al. (2017b), was used as a positive control in all the experiments carried out hereinafter. The recombinant CfPDIP1-elicited H_2O_2 accumulation profile showed that

CfPDIP1ΔN1-21 followed by CfPDIP1ΔN1-45 induced maximum levels of H_2O_2 on CoC 671 suspension cells, which was comparable to the positive controls, native CfPDIP1, and CfEPL1ΔN1-92 proteins (Fig. 7a). However, the quantity of H_2O_2 induced by the full length CfPDIP1 (CfPDIP1FL) was relatively far less than the other two CfPDIP1 proteins. An extracellular alkalinization assay also showed a relatively similar trend of defense elicitation, wherein CfPDIP1ΔN1-21 resulted in rapid alkalinization followed by CfPDIP1ΔN1-45 (Fig. 7b). Specifically, in both the assays, the level of defense response induced by CfPDIP1ΔN1-21 was slightly higher than the purified native CfPDIP1 protein but apparently lesser than CfEPL1ΔN1-92 protein. Besides, histochemical detection of the degree of H_2O_2 accumulation in suspension cells at 48 h after elicitation also showed a similar trend of defense elicitation by the recombinant domain deletional CfPDIP1 variants (Fig. 7c). Precisely, among the recombinant CfPDIP1 proteins, the maximum amount of brown precipitation was observed with CfPDIP1ΔN1-21, which was comparable with the native CfPDIP1 and CfEPL1ΔN1-92 proteins.

In contrary to the results of sugarcane suspension cell bioassays, which showed that CfPDIP1ΔN1-21 distinctively induced maximum degree of defense, HR assay on *N. tabacum* leaves showed that all the three recombinant CfPDIP1 proteins rapidly triggered HR (Fig. 8a). In fact, the magnitude and rate of HR development induced by these three recombinant proteins were on par with the native CfPDIP1 and CfEPL1ΔN1-92 proteins. Further, DAB staining of these infiltrated leaves at 24 hpi showed a distinctively higher production of H_2O_2 than the mock control (Fig. 8b). However, callose deposition assay revealed that the amount of callose deposits induced per unit area has significant variations among the three recombinant proteins (Fig. 8c). Particularly, the number of callose deposits observed in CfPDIP1ΔN1-21 was higher than the other two variants and native CfPDIP1 proteins, even though it was lesser than the positive control (CfEPL1ΔN1-92) in all the three replications (data not shown). Since CfPDIP1ΔN1-21 was found to trigger maximum defense responses among the three recombinant CfPDIP1 proteins in most of the bioassays, it was used for further defense priming efficacy-related experiments.

Effect of priming and co-infiltration of CfPDIP1ΔN1-21 on sugarcane leaves

To characterize the functional role of CfPDIP1ΔN1-21 during sugarcane-*C. falcatum* interaction, CfPDIP1ΔN1-21 primed and unprimed CoC 671 leaves were evaluated by detached leaf assay method by inoculating *C. falcatum* (*Cf*671) spores. Similarly, to assess the overexpression effect of CfPDIP1ΔN1-21 during host-pathogen interaction, unprimed CoC 671 leaves were co-infiltrated with CfPDIP1ΔN1-21 mixed *Cf*671 spores, in order to mimic overexpression. The results of these experiments showed that CfPDIP1ΔN1-21 priming has reduced the size of disease (lesion) development on par with the PAMP, CfEPL1ΔN1-92 (Fig. 9a and Table S4 in the supplementary material). However, the imitation of overexpression of CfPDIP1ΔN1-21 enhanced the rate of disease development, when compared to the unprimed pathogen inoculated control. Microscopic observations showed that the overexpression effect of CfPDIP1ΔN1-21 has intensified the number of appressorial structures (a specialized infection structure that facilitates penetration into the host cells), which in turn increased the rate of acervuli formations (an asexual fruiting body producing spores) (Fig. 9b and Table S4 in the supplementary material). On the other hand, a relatively smaller number of appressoria and very few pre-emergence stage acervuli were observed on CfPDIP1ΔN1-21 primed leaves. Overall, the priming and co-infiltration assays indicated that the CfPDIP1ΔN1-21 protein could indeed possess a distinct functional property, in addition to the properties of an elicitor.

Up-regulation of defense-related genes and concomitant suppression of disease severity in CfPDIP1ΔN1-21 primed canes

To evaluate the efficacy of CfPDIP1ΔN1-21 priming against red rot at molecular level, the biomass of *C. falcatum* and the concomitant expression of few important candidate defense-related genes were profiled at different time points (0, 12, 24, 48, 72, 120, 600 hpi) of host-pathogen interaction using qPCR. The pathogen biomass quantitation profiles which otherwise indicate the degree of pathogen colonization and disease severity showed a significant reduction in the amount of pathogen biomass in CfPDIP1ΔN1-21 primed canes, since 72 hpi (Fig. 10a). Interestingly, the degree of disease suppressive effect observed with CfPDIP1ΔN1-21 priming was on par with the priming with the PAMP, CfEPL1ΔN1-92.

Further, the expression of five potential candidate defense-related genes or putative defense markers, viz., nonexpressor of pathogenesis-related protein 1 (*ScNPR1*), isochorismate synthase (*ScICS*), β-1,3-glucanase D (*ScPR2*), chitinase VII (*ScPR3*), and defensin 5 genes were profiled (Fig. 10b–f). Interestingly, the expression profiles showed that all these five genes were up-regulated in response to CfPDIP1ΔN1-21 priming at 0 hpi (pre-inoculation stage). In other words, the basal expression of these genes was induced in response to priming, even before pathogen inoculation. More specifically, the expression of *ScICS* and *ScNPR1*, the master regulators of major defense pathways, was significantly up-regulated at the earlier time points (Fig. 10b, c). Similarly, the expression of *ScPR2*, *ScPR3*, and defensin 5 genes remained to be up-regulated until 48 hpi in CfPDIP1ΔN1-21 primed samples (Fig. 10d–f). Overall, the expression pattern of most of these

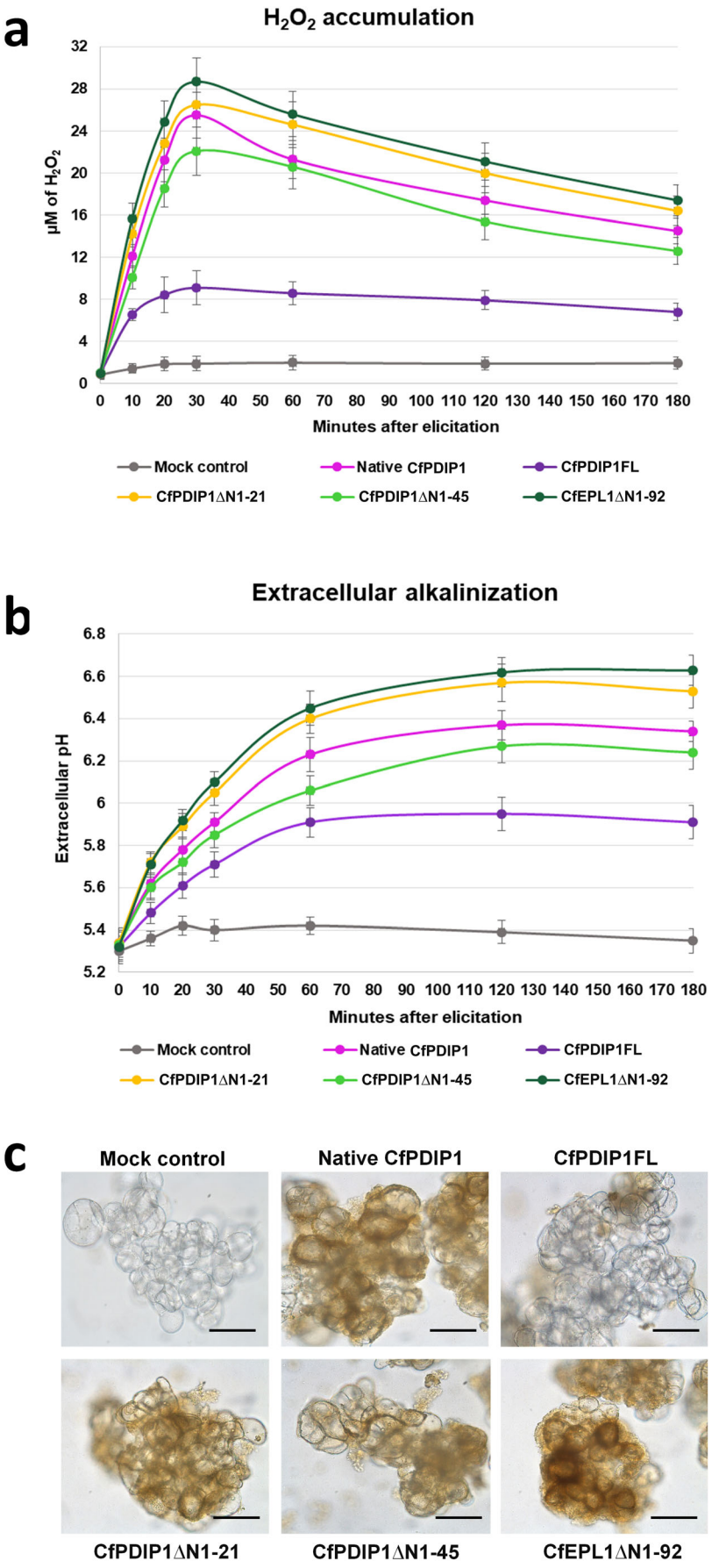

Fig. 7 Elicitation of sugarcane suspension cells (cv. CoC 671) with recombinant CfPDIP1 proteins. **a** Temporal accumulation profile of H_2O_2 in CoC 671 suspension cells after elicitation with recombinant CfPDIP1 proteins. **b** Induction of extracellular alkalinization by recombinant CfPDIP1 proteins. **c** Microscopic observation of H_2O_2 accumulation in CoC 671 suspension cells by DAB staining at 48 h after elicitation with recombinant CfPDIP1 proteins. Bar indicates 100 µm. For mock control, assay buffer was used. Native CfPDIP1 indicates purified native CfPDIP1 protein fraction. Purified recombinant CfEPL1ΔN1–92 protein (a PAMP) of *C. falcatum* was used as a positive control

defense genes in CfPDIP1ΔN1-21 was apparently similar to CfEPL1ΔN1-92 primed samples.

Discussion

Identifying the molecular determinants of plant-pathogen interactions, especially, PAMPs/elicitors, effectors, and R genes, is the key to elucidate the mechanisms of pathogenicity and disease resistance, which would aid in developing sustainable crop protection and improvement programs (Wirthmueller et al. 2013; Ashwin et al. 2017c). In this context, mining of secreted proteins through proteomic approaches is gaining more significance as it represents the functional biomolecules of living system (Ashwin et al. 2017c). Recently, we have analyzed the secretome profiles of light-cultured (high virulent) and dark-cultured (less virulent) *C. falcatum* by using two dimensional electrophoresis (2DE) coupled with MALDI TOF/TOF and found that CfEPL1 a well-conserved PAMP protein was highly abundant in the less virulent *C. falcatum*, whereas many pathogenicity-related proteins were highly abundant in the high virulent *C. falcatum* (Ashwin et al. 2017b). We further reported that the major cerato-platanin domain (CfEPL1ΔN1-92) of CfEPL1 protein was essential to induce systemic resistance in sugarcane.

In the present study, we systematically screened the in vitro secretome of *C. falcatum* (high virulent) using top-down approach, a strategy similar to the principle of molecular sieving to identify the protein(s) that could sensitize and trigger plant defense responses. A similar kind of top-down strategy was adopted by many researchers for more than a decade. For instance, the proteinaceous elicitors such as cerato-platanins (Pazzagli et al. 1999), PevD1 (Wang et al. 2012), and MoHrip1 (Chen et al. 2012) were purified from the culture filtrates of fungal pathogens, whereas the elicitors such as Sm1 (Djonovic et al. 2006) and AsES (Chalfoun et al. 2013) were purified from the culture filtrates of symbiotic plant microbes and saprophytes, respectively. This top-down strategy is in contrast to our previous study (Ashwin et al. 2017b), wherein the PAMP, CfEPL1 was characterized using a bottom-up approach.

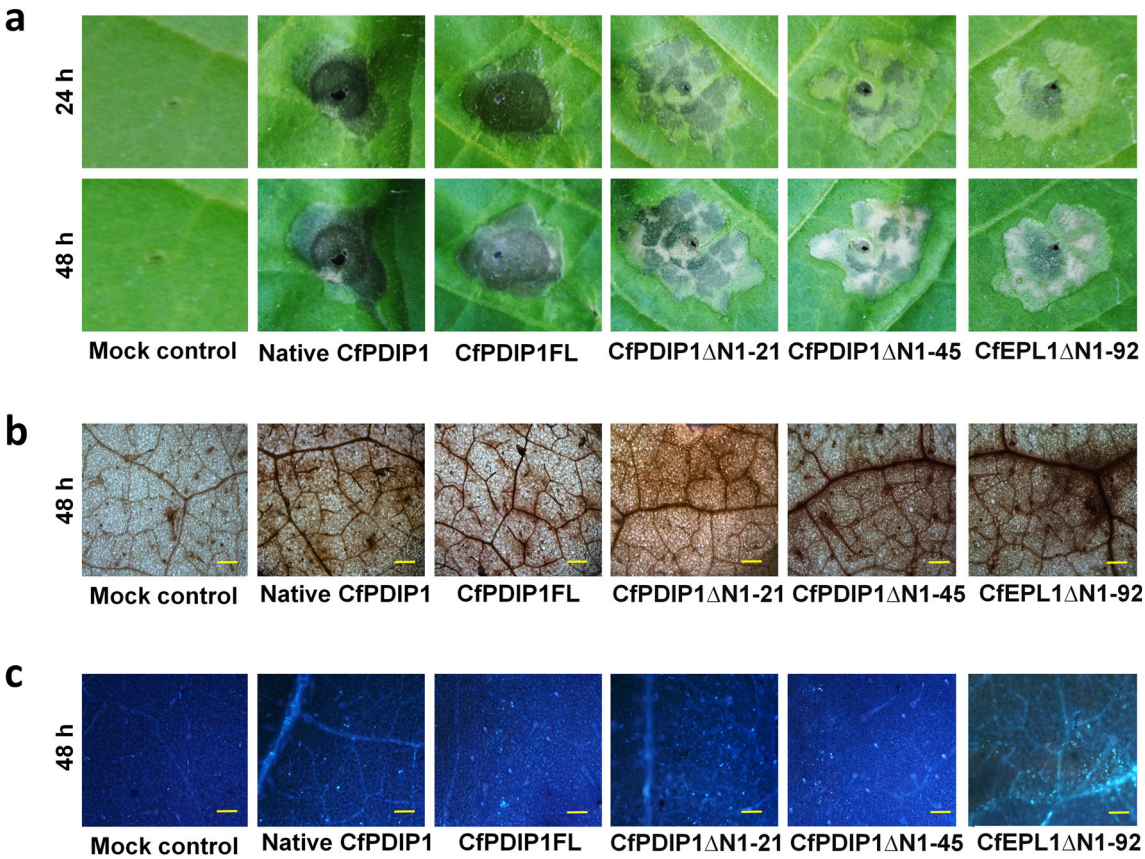

Fig. 8 Induction of defense responses by recombinant CfPDIP1 proteins on *N. tabacum* leaves. **a** Detection of HR induced by recombinant CfPDIP1 proteins in *N. tabacum* leaves at 24 and 48 h post-infiltration. **b** Microscopic observation of H_2O_2 accumulation in *N. tabacum* leaves by DAB staining at 24 h after infiltration with recombinant CfPDIP1 proteins. **c** Microscopic observation of recombinant CfPDIP1 proteins induced callose depositions (bright white spots) in *N. tabacum* leaves by aniline blue staining method at 24 h post infiltration. Bars indicate 100 μm. For mock control, assay buffer was used. Native CfPDIP1 indicates purified native CfPDIP1 protein fraction. Purified recombinant CfEPL1ΔN1-92 protein (a PAMP) of *C. falcatum* was used as a positive control

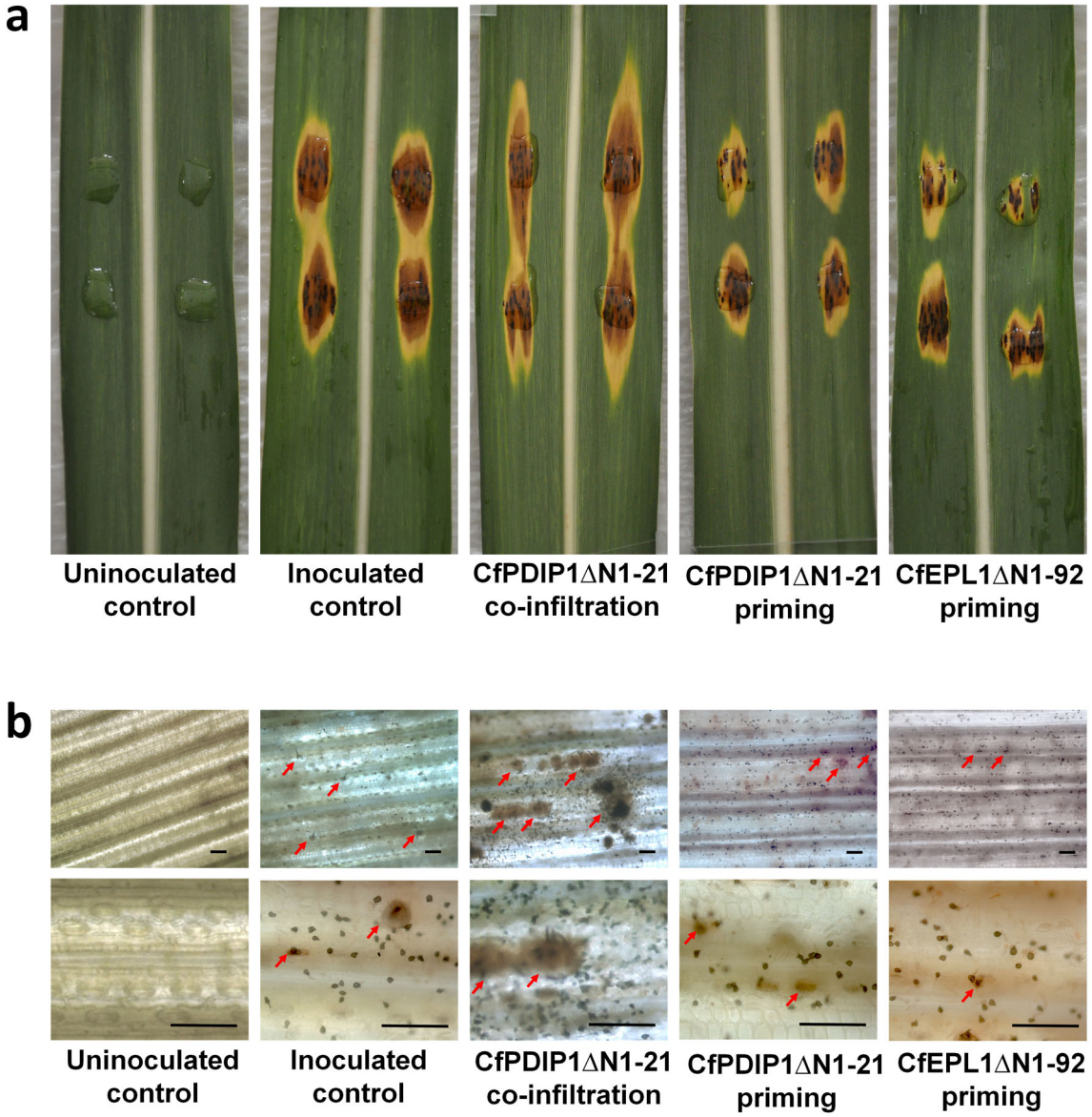

Fig. 9 Co-infiltration and priming effects of CfPDIP1ΔN1-21 on sugarcane leaves by detached leaf assay method. **a** Macroscopic observation of leaf bioassay at 72 h post-inoculation. Brown and yellow lesion indicates the extent of pathogen colonization and their consequent senescence effect, respectively. **b** Microscopic observation of leaf bioassay at 72 h post-inoculation. Bar indicates 50 μm. Red arrows indicate emerged and emerging acervuli structures whereas dark brown spots indicate appressorial structures of *C. falcatum*. Purified recombinant CfEPL1ΔN1-92 protein (a PAMP) of *C. falcatum* was used as a positive control

H_2O_2, the predominant nonradical of reactive oxygen species (ROS), is regarded as one of the important secondary messengers and sometimes as a primary messenger of defense signaling in plants against any stress and in response to the perception of various PAMPs (elicitors) and effectors (Møller and Sweetlove 2010). ROS production in turn triggers a complex network of defense signaling pathways to act against the perceived invasion through extracellular/apoplastic alkalinization, phytoalexin production, reinforcement of structural barriers like callose deposition in cell wall, programmed cell death (HR), etc. (Barna et al. 2012; Lehmann et al. 2015). Hence, in this study, the quantitative and qualitative analyses of H_2O_2 production and the observation of HR induction were considered as the indices of defense elicitation in the bioassays. Since our goal has been to shortlist the number of proteins to be screened in each step, the 10–30-kDa fraction that had less number of proteins but similar to other two active fractions on that range was selected for further screening. In subsequent fractionation and separation of 10–30 kDa fraction using AEC and SEC, a single protein of approximately 14 kDa protein that could trigger HR in *N. tabacum* leaves was purified.

Identification of this purified HR-inducing protein using MALDI TOF/TOF and subsequent in silico analysis revealed

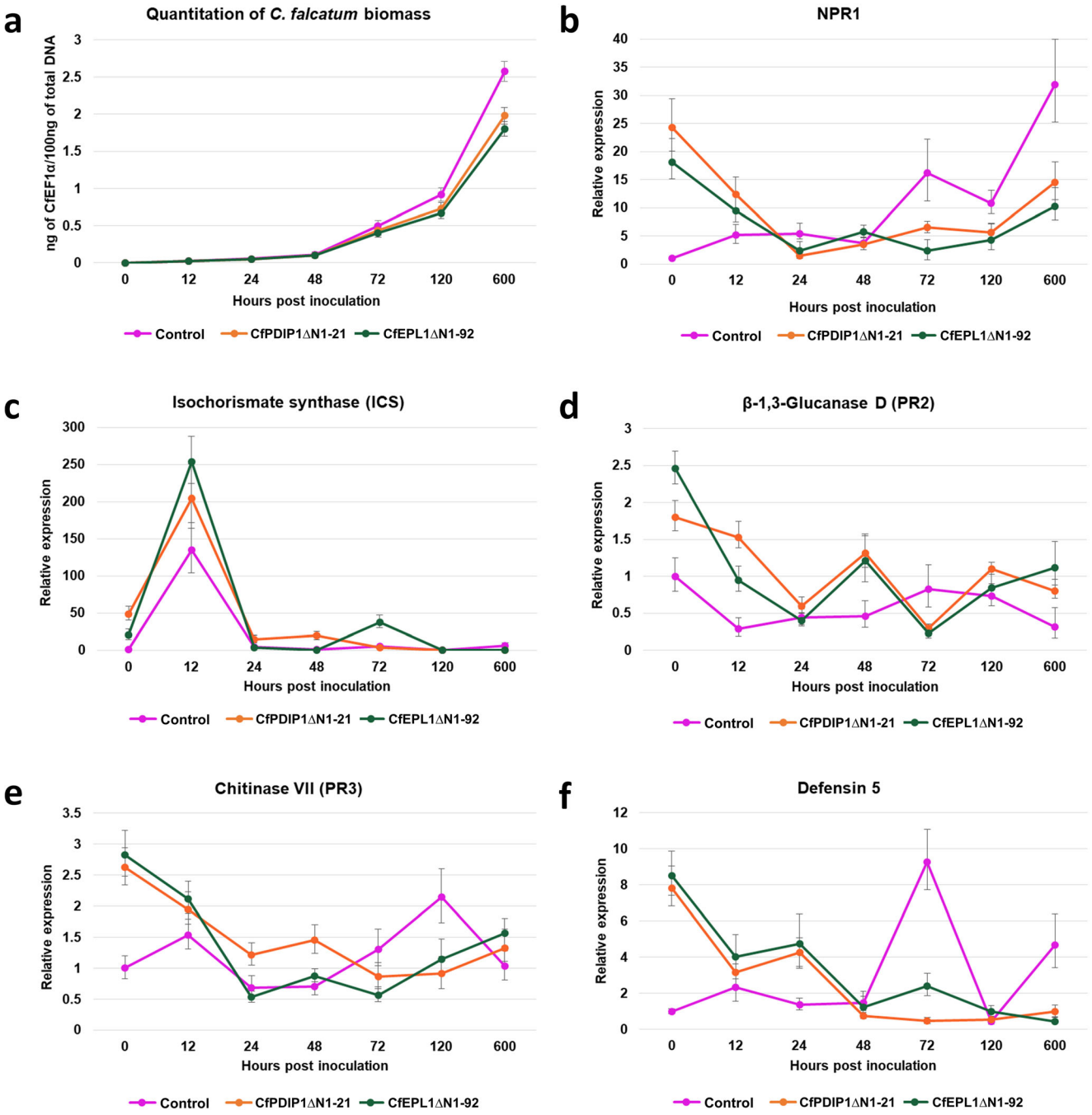

Fig. 10 Quantitation of *C. falcatum* biomass and relative expression analysis of potential candidate defense-related genes of CfPDIP1ΔN1-21 primed sugarcane stalks. "0 h" indicates primed mock inoculated control. Purified recombinant CfEPL1ΔN1-92 (a PAMP) primed canes were used as a positive control

that it is a novel hypothetical protein, discovered recently by us as one of the high abundant proteins in the secretome profile of high virulent *C. falcatum* with a provisional name of HYP2 (Ashwin et al. 2017b). Besides, in that previous study, we have reported a truncated isoform of this CfPDIP1 protein of approximately 10 kDa. However, an in-depth transcriptional expression analysis indicated that the isoform variation was only at the protein level and not due to alternative splicing as supposed to be due to unknown reasons. Hence, in the present study, the coverage of the peptide spectral matches (PSMs) was analyzed against the full length CfPDIP1 protein sequence derived from the *C. falcatum* database and found that the sequence of purified HR-inducing protein matched with the full length CfPDIP1 protein, excluding the predicted signal peptide region. Particularly, the PSMs have covered the truncated portion (21st–45th amino acids) of the second

isoform. Besides, the observed molecular weight of the HR-inducing protein closely matched with the high abundant CfPDIP1 protein than the truncated variant of CfPDIP1. With all these analyses, we have established that the HR-inducing protein identified in this study was the high abundant full length (except signal peptide) isoform of CfPDIP1 protein. Since the signal peptides of most of the classically secreted proteins get cleaved while passing through the membrane, the PSMs of HR-inducing protein did not cover the signal peptide region of the full length CfPDIP1 protein (Peberdy 1994; Emanuelsson et al. 2007).

EffectorP tool predicted that all the three variants (domain deletional) of CfPDIP1, viz., CfPDIP1FL (full length with signal peptide), CfPDIP1ΔN1-21 (full length without signal peptide), and CfPDIP1ΔN1-45 (the truncated isoform), have greater probability to be classified as effectors. However, transcriptional profiling showed that the expression of *CfPDIP1* in the compatible interaction was few folds lesser than the incompatible interaction, and the expression was constitutive throughout the phases of colonization. In general, *Colletotrichum* spp. follow three different models of hemibiotrophic colonization during their interaction with different hosts. Among the three, *C. falcatum* follows the *Colletotrichum graminicola* lifestyle model of intracellular hemibiotrophy, wherein which the biotrophy persists at the progressively colonizing cells, while the necrotrophy confined at the center of colonization (Crouch et al. 2014). The different phases of this lifestyle comprehend the initial infection phase that encompasses germination, appressorial formation, and penetration (0–24 h), a biotrophic phase that represents the formation of primary hyphae (24–48 h), and a necrotrophic phase that includes the brief transition from primary to secondary hypha and subsequent colonization of nearby cells (> 48 h) (O'Connell et al. 2012; Gan et al. 2012). Therefore, the ubiquitous expression of *CfPDIP1* has suggested that it could be an essential biomolecule of *C. falcatum* and might be required throughout its life span under both in vitro and in planta conditions, which substantiated the properties of a PAMP rather than the properties of an active secreted effector. However, the spike in the expression level of *CfPDIP1* at earlier stages of host-pathogen interaction than the axenic culture indicated that the CfPDIP1 protein may play a potential role in the dynamic host-pathogen interaction. Many filamentous fungi, including the *Colletotrichum* spp., do secrete a range of effector-like proteins even before the contact with plant surface or throughout the life cycle (O'Connell et al. 2012; Kleemann et al. 2012; Lanver et al. 2014; Guzman-Guzman et al. 2017). These kinds of proteins act like the hydrophobins or repellants and protect the hyphal structure from the attacks of the plant defense molecules during colonization (Ruocco et al. 2015; Lo presti et al. 2015). Altogether, the expression analyses have substantiated the elicitor properties of CfPDIP1 protein and necessitated an elaborate functional characterization.

In vitro expression and purification of three different domain deletional variants of CfPDIP1 showed that a certain quantity of the purified recombinant CfPDIP1ΔN1-21 and CfPDIP1ΔN1-45 proteins tends to assemble into dimeric and tetrameric forms. This assembling property has continued even after purification of their respective monomeric forms using SEC. Further, the increment of the concentration of reducing agents did not reduce them to their monomeric forms (data not shown). A similar phenomenon was also reported earlier with the recombinant CfEPL1 proteins of *C. falcatum* (Ashwin et al. 2017b). On the contrary, CfPDIP1FL protein did not form any dimeric or tetrameric forms. This was probably because of the presence of 21 residue signal peptide at the N-terminal end that might have prevented the formation such structures. Therefore, based on the results of dose optimization experiment, 50-μg/mL concentration of the purified recombinant proteins that had both dimeric and tetrameric forms was used for subsequent bioassays. For dose optimization, the maximum generation of H_2O_2 with minimum amount of cell death was used as the criteria because generally the degree of ROS production has been directly proportional to and associated with cell death (Wang et al. 2016; Chen et al. 2012, 2014). Moreover, it is recommended to use the minimal concentration of elicitors for host defense priming, as higher concentrations may have some detrimental effects on plant metabolism, which would also impact on fitness cost (Thakur and Sohal 2013; Martinez-Medina et al. 2016).

Functional bioassay of purified recombinant CfPDIP1 proteins on CoC 671 suspension cells indicated that only CfPDIP1ΔN1-21 followed by CfPDIP1ΔN1-45 triggered rapid extracellular alkalinization and maximum amount of H_2O_2 production. In contrast, CfPDIP1FL elicited only the least amount of defense responses. These observations suggested that the presence of the signal peptide in CfPDIP1FL might have either affected its function or hindered its perception as an elicitor in sugarcane. Unlike suspension cell assays, the bioassays on *N. tabacum* leaves such as HR assay and DAB staining of H_2O_2 did not show significant difference in the efficacy of defense elicitation among the CfPDIP1 variants. Only the callose deposition assay showed that the number of callose deposits in CfPDIP1ΔN1-21 was slightly higher than the other two variants. Here, the observed differential responses with respect to different hosts reinstate the fact that the perception of an elicitor and subsequent induction of defense, either PTI or effector-triggered immunity (ETI), are genotype-specific and may vary from plant to plant (Boller and Keen 1999; Thomma et al. 2011). Altogether, the functional characterization of the three domain deletional CfPDIP1 proteins indicated that the signal peptide region (1–21 residues) was dispensable, but the intermittent domain (22–45 residues) and the main domain (46–132 residues) were

essential for induction of maximum defense responses in sugarcane. Therefore, the variant CfPDIP1ΔN1-21 that comprises of both the intermittent as well as the main domains was used for further defense priming assays.

Disease suppressive effect observed with CfPDIP1ΔN1-21 priming on sugarcane leaves has substantiated the earlier reports stating that without the real-time confrontation of a pathogen, perception of PAMPs and certain effectors can activate host defense and promote resistance, which would help to overcome or suppress subsequent attack from the pathogen (Wiesel et al. 2014; Burketova et al. 2015). Even though the co-infiltration of CfPDIP1ΔN1-21 on unprimed leaves enhanced disease susceptibility, it cannot be attributed to the properties of an effector, because of its constitutive and higher expression during incompatible interaction. Similar effector-like properties have been reported with the secreted hydrophobins of many filamentous fungi. These cysteine-rich, constitutively secreted proteins are essential for attachment to different surfaces and play a major role in host-pathogen interactions (Guzman-Guzman et al. 2017). Presumably, CfPDIP1 may also have similar structural adhesion or formation related roles during the plant-pathogen interaction, in addition to the properties of being an elicitor. Nevertheless, further experiments like ectopic expression, deletion, and complementation of the CfPDIP1 gene only can decisively confirm whether CfPDIP1 may play the role of effector or not.

Quantitative assessment of pathogen biomass and transcriptional profiling of potential candidate defense markers (*ScNPR1*, *ScICS*, *ScPR2*, *ScPR3*, and defensin 5) indicated that CfPDIP1ΔN1-21 priming has indeed activated the host defense pathways even before the pathogen inoculation and resulted in the reduction in pathogen biomass in the distal stalk tissues. This otherwise indicated that the foliar priming has activated systemic resistance in stalk tissues and suppressed disease severity as in the case of the PAMP, CfEPL1ΔN1-92 during sugarcane-*C. falcatum* interaction (Ashwin et al. 2017b). Since the expression of *ScNPR1*, the master regulator of major defense-related pathways, is associated with the downstream expression of PR proteins and other defense-related proteins, the defense markers *ScPR2* (β-1,3-glucanase), *ScPR3* (chitinase VII), and defensin 5 might have got up-regulated in succession with *ScNPR1* expression (Pajerowska-Mukhtar et al. 2013; Ali et al. 2017).

Comprehensively, in this study, we report the purification and functional characterization of a novel secreted protein, CfPDIP1, which could act as an elicitor upon priming and might play an important role during the sugarcane-*C. falcatum* interaction. To our knowledge, this is the first study demonstrating the elicitation property of a novel class of protein from *Colletotrichum* spp. Since the novel CfPDIP1 protein was found to induce host resistance in a red rot susceptible sugarcane cultivar, CoC 671, the prospect of similar or even higher degree of defense elicitation effect in red rot resistant and field tolerant sugarcane cultivars is huge. On a futuristic perspective, the identification of the interacting partners of CfPDIP1 during in planta interaction would help to delineate the infection strategy of *C. falcatum* and would decipher the mechanism of PTI in sugarcane.

Acknowledgements The authors are grateful to The Director, ICAR-Sugarcane Breeding Institute for providing facilities and continuous encouragement. The financial support received from Department of Science and Technology (DST), New Delhi and Indian Council of Agricultural Research (ICAR), New Delhi is greatly acknowledged. Also, the financial support received from University Grants Commission (UGC), New Delhi in the form of NET-JRF fellowship by the first author is duly acknowledged. The authors are indebted to INPPO (http://www.inppo.com/) for their support and encouragement.

Funding The study was funded by Department of Science and Technology (DST), Government of India, New Delhi, India (Grant Sanction order number SR/SO/PS-22/2010) and Indian Council of Agricultural Research (ICAR), New Delhi, India.

Compliance with ethical standards

Conflict of interest All the authors declare that they have no conflict of interest.

Ethical approval This article does not contain any studies with human participants or animals performed by any of the authors.

References

Ali S, Mir ZA, Tyagi A, Mehari H, Meena R, Bhat JA, Yadav P, Papalou P, Rawat S, Grover A (2017) Overexpression of NPR1 in *Brassica juncea* confers broad spectrum resistance to fungal pathogens. Front Plant Sci 8:1693

Anil K, Das SN, Podile AR (2014) Induced defense in plants: a short overview. Proc Natl Acad Sci India Sect B Biol Sci 84:669–679. https://doi.org/10.1007/s40011-013-0279-2

Ashwin NMR, Barnabas EL, Ramesh Sundar A, Muthumeena M, Malathi P, Viswanathan R (2017a) Disease suppressive effects of resistance-inducing agents against red rot of sugarcane. Eur J Plant Pathol 149:285–297. https://doi.org/10.1007/s10658-017-1181-1

Ashwin NMR, Barnabas L, Ramesh Sundar A, Malathi P, Viswanathan R, Masi A, Agrawal GK, Rakwal R (2017b) Comparative secretome analysis of *Colletotrichum falcatum* identifies a cerato-platanin protein (EPL1) as a potential pathogen-associated molecular pattern (PAMP) inducing systemic resistance in sugarcane. J Proteome 169:2–20. https://doi.org/10.1016/j.jprot.2017.05.020

Ashwin NMR, Barnabas L, Ramesh Sundar A, Malathi P, Viswanathan R, Masi A, Agrawal GK, Rakwal R (2017c) Advances in proteomic technologies and their scope of application in understanding plant–pathogen interactions. J Plant Biochem Biotechnol 26:371–386. https://doi.org/10.1007/s13562-017-0402-1

Barna B, Fodor J, Harrach BD, Pogány M, Király Z (2012) The Janus face of reactive oxygen species in resistance and susceptibility of plants to necrotrophic and biotrophic pathogens. Plant Physiol Biochem 59:37–43. https://doi.org/10.1016/j.plaphy.2012.01.014

Barnabas L, Ashwin NMR, Kaverinathan K, Trentin AR, Pivato M, Sundar AR, Malathi P, Viswanathan R, Rosana OB,

Neethukrishna K, Carletti P, Arrigoni G, Masi A, Agrawal GK, Rakwal R (2016) Proteomic analysis of a compatible interaction between sugarcane and *Sporisorium scitamineum*. Proteomics 16: 1111–1122. https://doi.org/10.1002/pmic.201500245

Bindschedler LV, Minibayeva F, Gardner SL, Gerrish C, Davies DR, Bolwell GP (2001) Early signalling events in the apoplastic oxidative burst in suspension cultured French bean cells involve cAMP and Ca2+. New Phytol 151:185–194. https://doi.org/10.1046/j.1469-8137.2001.00170.x

Böhm H, Albert I, Fan L, Reinhard A, Nürnberger T (2014) Immune receptor complexes at the plant cell surface. Curr Opin Plant Biol 20C:47–54. https://doi.org/10.1016/j.pbi.2014.04.007

Boller T, Felix G (2009) A renaissance of elicitors: perception of microbe-associated molecular patterns and danger signals by pattern-recognition receptors. Annu Rev Plant Biol 60:379–406. https://doi.org/10.1146/annurev.arplant.57.032905.105346

Boller T, Keen NT (1999) Resistance genes and the perception and transduction of elicitor signals in host-pathogen interactions. In: Slusarenko AJ, Fraser RSS, Van Loon LC (eds) Mechanisms of resistance to plant diseases. Springer, Dordrecht, pp 189–229. https://doi.org/10.1007/978-94-011-3937-3_7

Boyd LA, Ridout C, O'Sullivan DM, Leach JE, Leung H (2013) Plant-pathogen interactions: disease resistance in modern agriculture. Trends Genet 29:233–240. https://doi.org/10.1016/j.tig.2012.10.011

Burketova L, Trda L, Ott PG, Valentova O (2015) Bio-based resistance inducers for sustainable plant protection against pathogens. Biotechnol Adv 33:994–1004. https://doi.org/10.1016/j.biotechadv.2015.01.004

Chalfoun NR, Grellet-Bournonville CF, Martínez-Zamora MG, Díaz-Perales A, Castagnaro AP, Díaz-Ricci JC (2013) Purification and characterization of AsES protein: a subtilisin secreted by *Acremonium strictum* is a novel plant defense elicitor. J Biol Chem 288:14098–14113. https://doi.org/10.1074/jbc.M112.429423

Chen M, Zeng H, Qiu D, Guo L, Yang X, Shi H, Zhou T, Zhao J (2012) Purification and characterization of a novel hypersensitive response-inducing elicitor from *Magnaporthe oryzae* that triggers defense response in rice. PLoS One 7:e37654. https://doi.org/10.1371/journal.pone.0037654

Chen M, Zhang C, Zi Q, Qiu D, Liu W, Zeng H (2014) A novel elicitor identified from *Magnaporthe oryzae* triggers defense responses in tobacco and rice. Plant Cell Rep 33:1865–1879. https://doi.org/10.1007/s00299-014-1663-y

Conrath U, Beckers GJM, Flors V, García Agustín P, Jakab G, Mauch F, Newman M-A, Pieterse CMJ, Poinssot B, Pozo MJ, Pugin A, Schaffrath U, Ton J, Wendehenne D, Zimmerli L, Mauch-Mani B (2006) Priming: getting ready for battle. Mol Plant-Microbe Interact 19:1062–1071. https://doi.org/10.1094/MPMI-19-1062

Conrath U, Beckers GJM, Langenbach CJG, Jaskiewicz MR (2015) Priming for enhanced defense. Annu Rev Phytopathol 53:97–119. https://doi.org/10.1146/annurev-phyto-080614-120132

Crouch J, O'Connell R, Gan P, Buiate E, Torres MF, Beirn L, Shirasu K, Vaillancourt L (2014) The genomics of *Colletotrichum*. In: Dean RA, Lichens-Park A, Kole C (eds) Genomics of plant-associated fungi: monocot pathogens. Springer-Verlag, Berlin Heidelberg, pp 69–102. https://doi.org/10.1007/978-3-662-44053-7_3

Davies DR, Bindschedler LV, Strickland TS, Bolwell GP (2006) Production of reactive oxygen species in *Arabidopsis thaliana* cell suspension cultures in response to an elicitor from *Fusarium oxysporum*: implications for basal resistance. J Exp Bot 57:1817–1827. https://doi.org/10.1093/jxb/erj216

Diguta CF, Rousseaux S, Weidmann S, Bretin N, Vincent B, Guilloux-Benatier M, Alexandre H (2010) Development of a qPCR assay for specific quantification of *Botrytis cinerea* on grapes. FEMS Microbiol Lett 313:81–87. https://doi.org/10.1111/j.1574-6968.2010.02127.x

Dixon M, Webb EC (1962) Enzyme fractionation by salting-out: a theoretical note. Adv Protein Chem 16:197–219. https://doi.org/10.1016/S0065-3233(08)60030-3

Djonovic S, Pozo MJ, Dangott LJ, Howell CR, Kenerley CM (2006) Sm1, a proteinaceous elicitor secreted by the biocontrol fungus *Trichoderma virens* induces plant defense responses and systemic resistance. Mol Plant-Microbe Interact 19:838–853. https://doi.org/10.1094/MPMI-19-0838

Du J, Verzaux E, Chaparro-Garcia A, Bijsterbosch G, Keizer LP, Zhou J, Liebrand TW, Xie C, Govers F, Robatzek S, Van Der Vossen EA (2015) Elicitin recognition confers enhanced resistance to *Phytophthora infestans* in potato. Nature Plants 1:15034. https://doi.org/10.1038/nplants.2015.34

Emanuelsson O, Brunak S, von Heijne G, Nielsen H (2007) Locating proteins in the cell using TargetP, SignalP and related tools. Nat Protoc 2:953–971. https://doi.org/10.1038/nprot.2007.131

Gan P, Ikeda K, Irieda H, Narusaka M, O'Connell RJ, Narusaka Y, Takano Y, Kubo Y, Shirasu K (2012) Comparative genomic and transcriptomic analyses reveal the hemibiotrophic stage shift of *Colletotrichum* fungi. New Phytol 197:1236–1249. https://doi.org/10.1111/nph.12085

Guzman-Guzman P, Aleman-Duarte MI, Delaye L, Herrera-Estrella A, Olmedo-Monfil V (2017) Identification of effector-like proteins in *Trichoderma* spp. and role of a hydrophobin in the plant-fungus interaction and mycoparasitism. BMC Genet 18:1–20. https://doi.org/10.1186/s12863-017-0481-y

Hamid S, Wong MY (2017) Elicitors and their roles in plant defence against pathogens particularly *Basidiomycetes*. In: Abdullah S, Chai-Ling H, Wagstaff C (eds) Crop improvement. Springer, Cham, pp 305–334. https://doi.org/10.1007/978-3-319-65079-1_14

Kleemann J, Rincon-Rivera LJ, Takahara H, Neumann U, van Themaat EVL, van der Does HC, Hacquard S, Stüber K, Will I, Schmalenbach W, Schmelzer E, O'Connell RJ, Ver Loren van Themaat E (2012) Sequential delivery of host-induced virulence effectors by appressoria and intracellular hyphae of the phytopathogen *Colletotrichum higginsianum*. PLoS Pathog 8:e1002643. https://doi.org/10.1371/journal.ppat.1002643

Lanver D, Berndt P, Tollot M, Naik V, Vranes M, Warmann T, Munch K, Rossel N, Kahmann R (2014) Plant surface cues prime *Ustilago maydis* for biotrophic development. PLoS Pathog 10:e1004272. https://doi.org/10.1371/journal.ppat.1004272

Lehmann S, Serrano M, L'Haridon F, Tjamos SE, Metraux JP (2015) Reactive oxygen species and plant resistance to fungal pathogens. Phytochemistry 112:54–62. https://doi.org/10.1016/j.phytochem.2014.08.027

Lo Presti L, Lanver D, Schweizer G, Tanaka S, Liang L, Tollot M, Zuccaro A, Reissmann S, Kahmann R (2015) Fungal effectors and plant susceptibility. Annu Rev Plant Biol 66:513–545. https://doi.org/10.1146/annurev-arplant-043014-114623

Martinez-Medina A, Flors V, Heil M, Mauch-Mani B, Pieterse CMJ, Pozo MJ, Ton J, Van Dam NM, Conrath U (2016) Recognizing plant defense priming. Trends Plant Sci 21:818–822. https://doi.org/10.1016/j.tplants.2016.07.009

Møller IM, Sweetlove LJ (2010) ROS signalling—specificity is required. Trends Plant Sci 15:370–374. https://doi.org/10.1016/j.tplants.2010.04.008

Muthiah M, Ramadass A, Amalraj RS, Palaniyandi M, Rasappa V (2013) Expression profiling of transcription factors (TFs) in sugarcane X *Colletotrichum falcatum* interaction. J Plant Biochem Biotechnol 22:286–294. https://doi.org/10.1007/s13562-012-0157-7

O'Connell RJ, Thon MR, Hacquard S, Amyotte SG, Kleemann J, Torres MF, Damm U, Buiate E, Epstein L, Alkan N, Altmüller J, Alvarado-Balderrama L, Bauser C, Becker C, Birren BW, Chen Z, Choi J, Crouch JA, Duvick JP, Farman M, Gan P, Heiman D, Henrissat B, Howard RJ, Kabbage M, Koch C, Kracher B, Kubo Y, Law AD, Lebrun M-H, Lee Y-H, Miyara I, Moore N, Neumann U, Nordström

K, Panaccione DG, Panstruga R, Place M, Proctor RH, Prusky D, Rech G, Reinhardt R, Rollins J, Rounsley S, Schardl CL, Schwartz DC, Shenoy N, Shirasu K, Sikhakolli UR, Stüber K, Sukno S, Sweigard J, Takano Y, Takahara H, Trail F, van der Does HC, Voll LM, Will I, Young S, Zeng Q, Zhang J, Zhou S, Dickman MB, Schulze-Lefert P, Ver Loren van Themaat E, Ma L-J, Vaillancourt LJ (2012) Lifestyle transitions in plant pathogenic *Colletotrichum* fungi deciphered by genome and transcriptome analyses. Nat Genet 44:1060–1065. https://doi.org/10.1038/ng.2372

Pajerowska-Mukhtar KM, Emerine DK, Mukhtar MS (2013) Tell me more: roles of NPRs in plant immunity. Trends Plant Sci 18:402–411. https://doi.org/10.1016/j.tplants.2013.04.004

Pazzagli L, Cappugi G, Cappugi G, Manao G, Manao G, Camici G, Camici G, Santini A, Santini A, Scala A (1999) Purification, characterization, and amino acid sequence of cerato-platanin, a new phytotoxic protein from *Ceratocystis fimbriata* f. sp. *platani*. Mol Biol 274:24959–24964. https://doi.org/10.1074/jbc.274.35.24959

Peberdy JF (1994) Protein secretion in filamentous fungi-trying to understand a highly productive black box. Trends Biotechnol 12:50–57. https://doi.org/10.1016/0167-7799(94)90100-7

Prasanth CN, Viswanathan R, Krishna N, Malathi P, Ramesh Sundar A, Tiwari T (2017) Unraveling the genetic complexities in gene set of sugarcane red rot pathogen *Colletotrichum falcatum* through transcriptomic approach. Sugar Tech 19:604–615. https://doi.org/10.1007/s12355-017-0529-3

Ramesh Sundar A, Velazhahan R, Nagarathinam S, Vidhyasekaran P (2008) Induction of pathogenesis-related proteins in sugarcane leaves and cell-cultures by a glycoprotein elicitor isolated from *Colletotrichum falcatum*. Biol Plant 52:321–328. https://doi.org/10.1007/s10535-008-0066-8

Ramesh Sundar A, Vidhyasekaran P (2003) Differential induction of phenylpropanoid metabolites in suspension cultured cells of sugarcane by fungal elicitors. Acta Phytopathol Entomol Hungarica 38:29–42. https://doi.org/10.1556/APhyt.38.2003.1-2.5

Ramesh Sundar A, Viswanathan R, Nagarathinam S (2009) Induction of systemic acquired resistance (SAR) using synthetic signal molecules against *Colletotrichum falcatum* in sugarcane. Sugar Tech 11:274–281. https://doi.org/10.1007/s12355-009-0047-z

Ruocco M, Lanzuise S, Lombardi N, Woo SL, Vinale F, Marra R, Varlese R, Manganiello G, Pascale A, Scala V, Turrà D, Scala F, Lorito M (2015) Multiple roles and effects of a novel *Trichoderma* hydrophobin. Mol Plant-Microbe Interact 28:167–179. https://doi.org/10.1094/MPMI-07-14-0194-R

Selvaraj N, Ramadass A, Amalraj RS, Palaniyandi M, Rasappa V (2014) Molecular profiling of systemic acquired resistance (SAR)-responsive transcripts in sugarcane challenged with *Colletotrichum falcatum*. Appl Biochem Biotechnol 174:2839–2850. https://doi.org/10.1007/s12010-014-1230-6

Shao M, Wang J, Dean RA, Lin Y, Gao X, Hu S (2008) Expression of a harpin-encoding gene in rice confers durable nonspecific resistance to *Magnaporthe grisea*. Plant Biotechnol J 6:73–81. https://doi.org/10.1111/j.1467-7652.2007.00304.x

Singh RP, Lal S (2000) Red rot. In: Rott P, Bailey RA, Comstock JC, Croft BJ, Girard JC, Saumtally AS (eds) A guide to sugarcane diseases. CIRAD Publication Services, Montpellier, pp 153–160

Sperschneider J, Gardiner DM, Dodds PN, Tini F, Covarelli L, Singh KB, Manners JM, Taylor JM (2016) EffectorP: predicting fungal effector proteins from secretomes using machine learning. New Phytol 210:743–761. https://doi.org/10.1111/nph.13794

Sundar AR, Ashwin NMR, Barnabas EL, Malathi P, Viswanathan R (2015) Disease resistance in sugarcane—an overview. Sci Agrar Parana 14:200–212. https://doi.org/10.18188/1983-1471/sap.v14n4p200-212

Takakura Y, Che FS, Ishida Y, Tsutsumi F, Kurotani KI, Usami S, Isogai A, Imaseki H (2008) Expression of a bacterial flagellin gene triggers plant immune responses and confers disease resistance in transgenic rice plants. Mol Plant Pathol 9:525–529. https://doi.org/10.1111/j.1364-3703.2008.00477.x

Thakur M, Sohal BS (2013) Role of elicitors in inducing resistance in plants against pathogen infection: a review. ISRN Biochem 2013:762412. https://doi.org/10.1155/2013/762412

Thomma BPHJ, Nürnberger T, Joosten MHAJ (2011) Of PAMPs and effectors: the blurred PTI-ETI dichotomy. Plant Cell 23:4–15. https://doi.org/10.1105/tpc.110.082602

Viswanathan R (2012) Sugarcane diseases and their management. ICAR-Sugarcane Breeding Institute, Coimbatore

Viswanathan R (2017) Pathogen virulence in sugarcane red rot pathogen versus varieties in cultivation: classical case of loss in virulence in the pathotype CF06 (*Cf*671). Sugar Tech 19:293–299. https://doi.org/10.1007/s12355-016-0458-6

Viswanathan R, Mohanraj D, Padmanaban P (1998) Comparison of three testing methods for evaluation of resistance to red rot caused by *Colletotrichum falcatum* in sugarcane (*Saccharum officinarum*). Indian J Agric Sci 68:226–230

Walters DR, Ratsep J, Havis ND (2013) Controlling crop diseases using induced resistance: challenges for the future. J Exp Bot 64:1263–1280. https://doi.org/10.1093/jxb/ert026

Wang B, Yang X, Zeng H, Liu H, Zhou T, Tan B, Yuan J, Guo L, Qiu D (2012) The purification and characterization of a novel hypersensitive-like response-inducing elicitor from *Verticillium dahliae* that induces resistance responses in tobacco. Appl Microbiol Biotechnol 93:191–201. https://doi.org/10.1007/s00253-011-3405-1

Wang Y, Wu J, Kim SG, Tsuda K, Gupta R, Park S-Y, Kim ST, Kang KY (2016) *Magnaporthe oryzae*-secreted protein MSP1 induces cell death and elicits defense responses in rice. Mol Plant-Microbe Interact 29:299–312. https://doi.org/10.1094/MPMI-12-15-0266-R

Wiesel L, Newton AC, Elliott I, Booty D, Gilroy EM, Birch PRJ, Hein I (2014) Molecular effects of resistance elicitors from biological origin and their potential for crop protection. Front Plant Sci 5:655. https://doi.org/10.3389/fpls.2014.00655

Wingfield PT (2016) Protein precipitation using ammonium sulfate. Curr Protoc Protein Sci 84:A.3F.1–A.3F.9. https://doi.org/10.1002/0471140864.psa03fs84

Wirthmueller L, Maqbool A, Banfield MJ (2013) On the front line: structural insights into plant-pathogen interactions. Nat Rev Microbiol 11:761–776. https://doi.org/10.1038/nrmicro3118

Yang Y, Zhang H, Li G, Li W, Wang X, Song F (2009) Ectopic expression of MgSM1, a Cerato-platanin family protein from *Magnaporthe grisea*, confers broad-spectrum disease resistance in *Arabidopsis*. Plant Biotechnol J 7:763–777. https://doi.org/10.1111/j.1467-7652.2009.00442.x

Zhang J, Zhou J-M (2010) Plant immunity triggered by microbial molecular signatures. Mol Plant 3:783–793. https://doi.org/10.1093/mp/ssq035